Palaeogeography, Palaeoclimatology, Palaeoecology 437 (2015) 165–180

Contents lists available at ScienceDirect

Palaeogeography, Palaeoclimatology, Palaeoecology

journal homepage: www.elsevier.com/locate/palaeo

Disentangling the history of complex multi-phased shell beds based on the analysis of 3D point cloud data

Mathias Harzhauser [a,*], Ana Djuricic [a,b], Oleg Mandic [a], Martin Zuschin [c], Peter Dorninger [a,d], Clemens Nothegger [a,d], Balázs Székely [b,e], Eetu Puttonen [f], Gábor Molnár [b,g], Norbert Pfeifer [b]

[a] Geological Paleontological Department, Natural History Museum Vienna, Vienna, Austria
[b] Department of Geodesy and Geoinformation, Research Group for Photogrammetry, Vienna University of Technology, Vienna, Austria
[c] Department of Palaeontology, University of Vienna, Vienna, Austria
[d] 4D-IT GmbH, Vienna, Austria
[e] Department of Geophysics and Space Science, Eötvös University, Budapest, Hungary
[f] Finnish Geospatial Research Institute in the National Land Survey of Finland, Department of Remote Sensing and Photogrammetry and Centre of Excellence in Laser Scanning Research, Geodeetinrinne 2, Masala FI-02431, Finland
[g] MTA-ELTE Geological, Geophysical and Space Science Research Group, Hungarian Academy of Sciences at Eötvös University, Budapest, Hungary

ARTICLE INFO

Article history:
Received 16 April 2015
Received in revised form 14 July 2015
Accepted 20 July 2015
Available online 1 August 2015

Keywords:
Terrestrial laser scanning
Oyster biostrome
Miocene
Taphonomy
Tsunami

ABSTRACT

We present the largest GIS-based data set of a single shell bed, comprising more than 10,280 manually outlined objects. The data are derived from a digital surface model based on high-resolution terrestrial laser scanning (TLS) and orthophotos obtained by photogrammetric survey, with a sampling distance of 1 mm and 0.5 mm, respectively. The shell bed is an event deposit, formed by a tsunami or an exceptional storm in an Early Miocene estuary. Disarticulated shells of the giant oyster *Crassostrea gryphoides* are the most frequent objects along with venerid, mytilid and solenid bivalves and potamidid gastropods. The contradicting ecological requirements and different grades of preservation of the various taxa mixed in the shell bed, along with a statistical analysis of the correlations of occurrences of the species, reveal an amalgamation of at least two pre- and two post-event phases of settlement under different environmental conditions. Certain areas of the shell bed display seemingly significant but opposing shell orientations. These patterns in coquinas formed by densely spaced elongate shells may result from local alignment of neighboring valves due to occasional events and bioturbation during the years of exposure. Similarly, the patchy occurrence of high ratios of shells in stable convex-up positions may simply be a result of such "maturity" effects. Finally, we document the difficulties in detecting potential tsunami signatures in shallow marine settings even in exceptionally preserved shell beds due to taphonomic bias by post-event processes.

1. Introduction

Shell beds are key features in sedimentary records throughout the Phanerozoic. The interplay between burial rates and population productivity is reflected in distinct degrees of shelliness (Tomašových et al., 2006; Patzkowsky and Holland, 2012). Consequently, shell beds may provide information on various physical processes that led to the accumulation and preservation of hard parts. Many shell beds pass through a complex history of formation being shaped by more than one factor (Kidwell, 1986, 1991; Fürsich and Oschmann, 1993; Mandic et al., 2004a; Zuschin et al., 2005, 2007). In shallow marine settings, the composition of shell beds is often strongly influenced by winnowing, reworking and transport. These processes may accumulate specimens that lived thousands of years apart (Kidwell and Tomašových, 2013 and references therein). A major obstacle in interpreting shell beds is the amalgamation of several depositional units in a single concentration, as is typical for tempestites and tsunamites. Disentangling such mixed assemblages requires understanding the ecological requirements of the taxa involved – which is achievable for geologically young shell beds with living relatives – and a statistical approach to quantify the contribution by the various death assemblages. Furthermore, it requires understanding the sedimentary processes potentially involved in their formation.

Here we present the first attempt to describe and decipher such a multi-phase shell bed based on a high-resolution digital surface model

* Corresponding author. Tel.: +43 1 52177 250; fax: +43 1 52177 459.
E-mail addresses: mathias.harzhauser@nhm-wien.ac.at (M. Harzhauser), ana.djuricic@geo.tuwien.ac.at (A. Djuricic), oleg.mandic@nhm-wien.ac.at (O. Mandic), martin.zuschin@univie.ac.at (M. Zuschin), p.dorninger@4d-it.com (P. Dorninger), c.nothegger@4d-it.com (C. Nothegger), balazs.szekely@ttk.elte.hu (B. Székely), eetu.puttonen@nls.fi (E. Puttonen), molnar@sas.elte.hu (G. Molnár), Norbert.pfeifer@geo.tuwien.ac.at (N. Pfeifer).

http://dx.doi.org/10.1016/j.palaeo.2015.07.038

(DSM) with a resolution of 1 mm combined with orthophotos with a nominal resolution of 0.5 mm per pixel. The shell accumulation covers an area of 27 × 17 m (459 m^2) with about 54,000 specimens, which were excavated at Stetten in Lower Austria (Fig. 1). Formed in an Early Miocene estuary of the Paratethys Sea, the shell bed is mainly composed of shells of the giant oyster *Crassostrea gryphoides* along with numerous other bivalves, gastropods and barnacles. This *Crassostrea* shell bed is the world's largest excavated fossil oyster biostrome and is a highlight of the geo-edutainment park "Fossilienwelt Weinviertel" (www.fossilienwelt.at/).

The term oyster reef is well established in estuarine ecology (e.g.: Powell et al., 2006; Thomsen et al., 2007; Lejart and Hily, 2011; van der Zee et al., 2012). Herein, we prefer to use the term biostrome of Lahee (1932) because many intertidal oyster bioconstructions lack a strong vertical growth component.

2. Geological setting and paleoenvironment

The Stetten site (48° 22′ 03.33 N, 16° 21′ 33.22 E) is part of the small Austrian Korneuburg Basin (KB), which is a half graben that formed within the Alpine-Carpathian thrust belt. This basin is about 20 km long and attains a maximum width of 7 km, but it is strongly narrowed in its northern extension (Wessely, 1998). The investigated oyster biostrome is the upper part of an about 600-m-thick siliciclastic succession of the Korneuburg Formation in the southern basin, which is tilted ca. 25° in the western direction (Fig. 2). Sand packages with trough cross-bedded sets are interpreted as tidal sand waves of the shoreface. Pelitic sediments mostly show even lamination to wavy bedding or thinly alternating sandy and muddy layers, indicative of tidal flat deposits (Zuschin et al., 2014). These deposits were dated into nannoplankton zone NN4, paleomagnetic chron C5C and mammal zone MN5 (Harzhauser and Wessely, 2003) corresponding to the latest Early Miocene (Burdigalian; Karpatian regional stage, ~16.2 Ma.).

A comprehensive data set on the fauna and flora of KB was published by Sovis and Schmid (1998, 2002). Additional details on ecology, climate and water chemistry were provided by Latal et al. (2005, 2006), Kern et al. (2010), Zuschin et al. (2004, 2014) and Harzhauser et al. (2007, 2010). A popular synthesis of the paleoenvironment is given in Harzhauser et al. (2009). According to these paleontological and geochemical data, the southern part of the basin was an estuarine ecosystem that existed for more than 700,000 years due to its peculiar tectonic setting and significant subsidence (Harzhauser et al., 2002; Latal et al., 2005, 2006; Zuschin et al., 2014). The foraminifera and mollusc faunas were partly adapted to brackish water conditions and

Fig. 2. The shell bed in the geo-edutainment during the terrestrial laser scanning campaign, showing the post-sedimentary tilting in the western direction.

indicate a very shallow water environment, with a maximum water depth of about 30 m (Rögl, 1998; Harzhauser et al., 2002). Along the seaward fringe, an *Avicennia* mangrove was established. Tidal mudflats and sandbars were settled by vast *Crassostrea* biostromes. These "reefs" became established in the mixohaline shallow subtidal to lower intertidal zone of the estuarine bay. Brackish marshes, shallow lakes, oxbows and rivers developed as the typical wetland types of the southern Korneuburg Basin (Harzhauser et al., 2002; Kern et al., 2010). A diverse mammalian fauna lived in the swamps and forests (Daxner-Höck, 1998). Palynological analyses by Kern et al. (2010) revealed a subtropical climate with mean annual temperatures between 15.7 and 20.8 °C.

3. Taxonomic inventory and autecology

During the excavations of the biostrome in 2005 and 2008, a detailed taxonomic survey of the macrofauna (>5 mm) was conducted, yielding an inventory of 46 molluscan species, comprising 23 gastropod, 1 cephalopod and 22 bivalve species (Table 1). The abundances of these taxa were categorized semi-quantitatively as *rare* (<10 specimens), *common* (10–100 specimens) and *frequent* (>100 specimens) in relation to the total excavation area of 459 m^2 (each bivalve shell counted as an individual). The most frequent gastropod species are the neritid *Nerita plutonis* (Basterot, 1825), the potamidid *Ptychopotamides papaveraceus* (Basterot, 1825), the calyptraeids *Calyptraea depressa* Lamarck, 1822 and *Calyptraea irregularis* (Cossmann and Peyrot, 1919), the naticid *Polinices pseudoredemptus* (Friedberg, 1911–28) and the nassariid *Nassarius edlaueri* (Beer-Bistrický, 1958). Among the bivalves, only 5 species are common to frequent: *C. gryphoides* (Schlotheim, 1813), *Perna aquitanica* (Mayer, 1858), *Ostrea digitalina* Dubois de Montpereux,

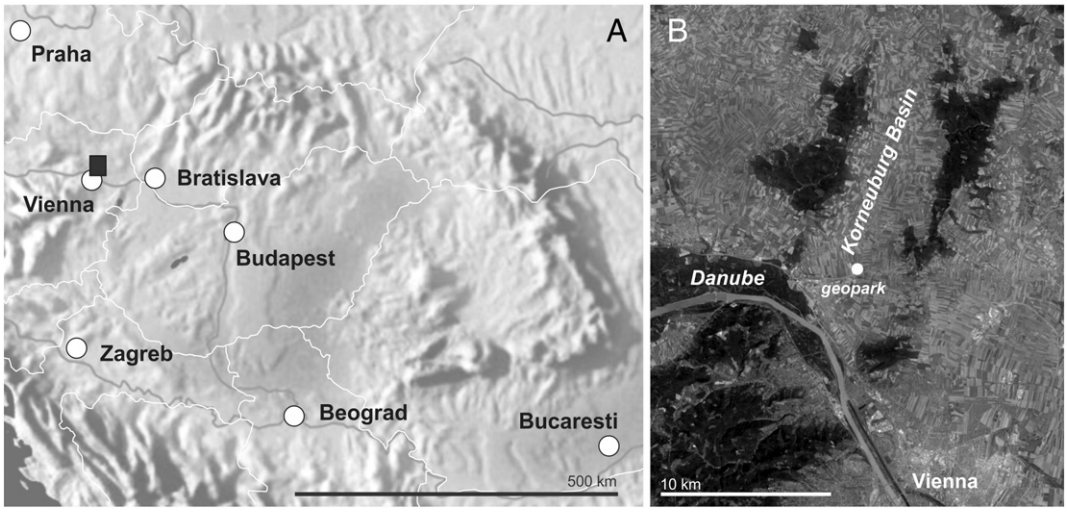

Fig. 1. Geographic setting of the Korneuburg Basin in Austria at the junction between the Alps and the Carpathians (A) and position of the site north of Vienna (B); map corresponds to black rectangle in A.

Table 1
List of marine species detected in the shell bed during excavation; these data are semi-quantitative; r—rare (<10 specimens), c—common (10–100 specimens), f—frequent (>100 specimens).

Class: Gastropoda Cuvier, 1795		
Superfamily: Trochoidea Rafinesque, 1815		
	Paroxystele amedei (Brongniart, 1823)	r
Superfamily: Neritoidea Rafinesque, 1815		
	Agapilia pachii	c
	Nerita plutonis (Basterot, 1825)	f
Superfamily: Cerithoidea Férussac, 1821–1822		
	Ptychopotamides papaveraceus (Basterot, 1825)	f
	Granulolabium bicinctum (Brocchi, 1814)	r
	Turritella gradata (Hörnes, 1856)	r
	Oligodia bicarinata (Eichwald, 1830)	r
	Petaloconchus intortus (Lamarck, 1822)	c
Superfamily: Calyptraeoidea Lamarck, 1822		
	Calyptraea depressa (Lamarck, 1822)	f
	Calyptraea irregularis (Cossmann & Peyrot, 1919)	f
Superfamily: Velutinoidea Gray, 1840		
	Erato sp.	r
Superfamily: Naticoidea Guilding, 1834		
	Polinices pseudoredemptus (Friedberg, 1923)	f
	Neverita josephinia (Risso, 1826)	r
Superfamily: Muricoidea Rafinesque, 1815		
	Ocenebra crassilabiata (Hilber, 1879)	c
	Ocinebrina striata (Eichwald, 1853)	c
	Janssenia echinulata (Pusch, 1837)	r
	Nassarius edlaueri (Beer-Bistricky, 1958)	f
	Cyllenina suessi (Hoernes and Auinger, 1882)	c
	Tudicla rusticula (Basterot, 1825)	c
Superfamily: Cancellariidae Forbes and Hanley, 1851		
	Solatia exwestiana (Sacco, 1894)	r
Superfamily: Conoidea Rafinesque, 1815		
	Perrona semimarginata (Lamarck, 1822)	r
	Perrona louisae (Hoernes and Auinger, 1891)	r
	Perrona vindobonensis (Hörnes, 1854)	r
Class: Cephalopoda Cuvier, 1795		
	Aturia aturi (Basterot, 1825)	r
Class: Bivalvia Linnaeus, 1758		
Superfamily: Gastrochaenoidea Gray, 1840		
	Rocellaria dubia (Pennant, 1777)	r
Superfamily: Arcoidea Lamarck, 1809		
	Anadara diluvii (de Lamarck, 1805)	r
Superfamily: Limopsoidea Dall, 1895		
	Glycymeris deshayesi (Mayer, 1868)	r
Superfamily: Mytiloidea Rafinesqe, 1815		
	Perna aquitanica (Mayer, 1858)	f
	Septifer oblitus (Michelotti, 1847)	r
Superfamily: Pteriidae Gray, 1847		
	Isognomon soldanii (Deshayes, 1836)	r
Superfamily: Pectinoidea Rafinesqe, 1815		
	Pecten styriacus (Hilber, 1879)	r
	Aequipecten macrotis (Sowerby in Smith, 1847)	r
Superfamily: Anomioidea Rafinesque, 1815		
	Anomia ephippium Linnaeus, 1758	r
Superfamily: Ostreoidea Rafinesque, 1815		
	Crassostrea gryphoides (Schlotheim, 1813)	f
	Ostrea digitalina (Dubois de Montpereux, 1831)	f
Superfamily: Lucinoidea Fleming, 1828		
	Loripes dujardini (Deshayes, 1850)	r
	Megaxinus incrassatus (Dubois de Montpereux, 1831)	r
	Diplodonta rotundata (Montagu, 1803)	r
Superfamily: Chamoidea Lamarck, 1822		
	Pseudochama gryphina (Lamarck, 1819)	r
Superfamily: Cardioidea Lamarck, 1809		
	Cardium hians (Brocchi, 1814)	
	Acanthocardia paucicostata (Sowerby, 1839)	f
Superfamily: Mactroidea Lamarck, 1809		
	Ervilia pusilla (Philippi, 1836)	r
Superfamily: Solenoidea Lamarck, 1809		
	Solen marginatus (Pulteney, 1799)	c
Superfamily: Tellinoidea de Blainville, 1814		
	Tellina planata (Linnaeus, 1758)	r
Superfamily: Veneroidea Rafinesque, 1815		
	Cordiopsis islandicoides (Lamarck, 1818)	r
	Venerupis basteroti (Mayer, 1857)	f

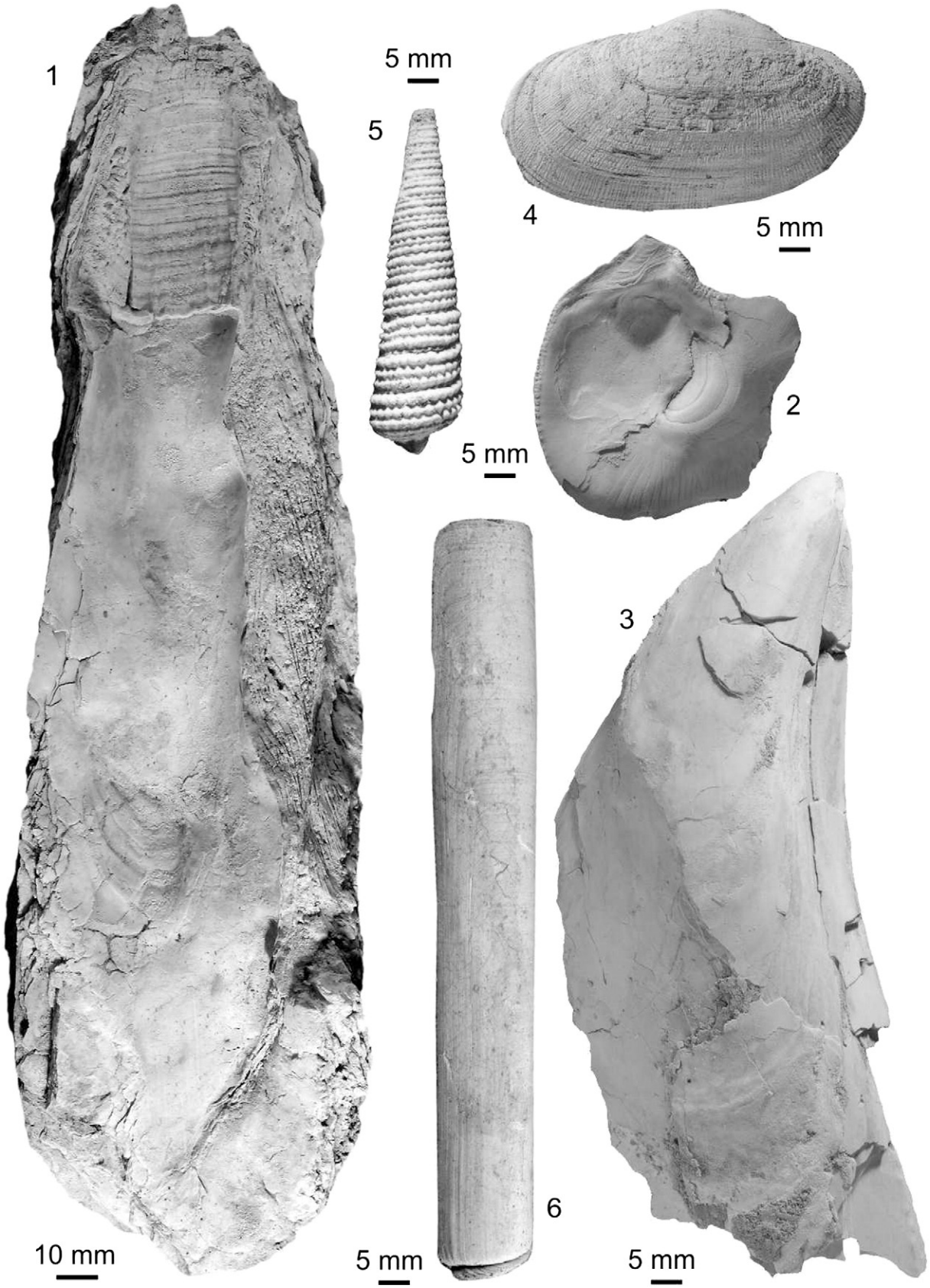

Fig. 3. Taxa analyzed herein: (1) *Crassostrea gryphoides* (Schlotheim, 1813), (2) *Ostrea digitalina* Dubois de Montpereux, 1831, (3) *P. aquitanica* (Mayer, 1858), (4) *Venerupis basteroti* (Mayer, 1857), (5) *Ptychopotamides papaveraceus* (Basterot, 1825), (6) *Solen marginatus* Pulteney, 1799.

1831, *Venerupis basteroti* (Mayer, 1857) and *Solen marginatus* Pulteney, 1799 (Fig. 3); the other species are rare. Similarly, the single cephalopod species *Aturia aturi* (Basterot, 1825) is represented by only a few specimens. Further, important constituents of the macroscopic invertebrate inventory are balanids and traces of clionid sponges, all of which are found mainly associated with *Crassostrea* shells. The following species have been analyzed quantitatively and qualitatively based on the DSM:

Crassostrea gryphoides (Fig. 3/1): calcitic shells of highly variable but generally strongly elongate shape; all shells are disarticulated. All taphonomic grades, from complete to highly fragmented and abraded, are present. This species can attain a length of up to 80 cm (Harzhauser et al., 2010). Like its extant congeners, *C. gryphoides* was a filter feeder adapted to strong fluctuations in salinity within the intertidal zone (Kennedy et al., 1996). In contrast to recent relatives, which settle preferably on living or dead conspecific shells (Coen and Luckenbach, 2000; Whitman and Reidenbach, 2012; Chinzei, 2013; George et al., 2015), this bivalve species apparently lived as a secondary soft-bottom dweller in a mixed mode of shell-supported reclining and mud sticking (sensu Seilacher et al., 1985; Seilacher and Gishlick, 2014). When found *in situ* with articulated valves in patches or small biostromes, *C. gryphoides* is associated with pelitic sediments or muddy sand. A similar situation was documented from a Burdigalian mudflat in the Mut Basin (Turkey) by Mandic et al. (2004a) and from the Miocene Rhône Basin in France by Laurain (1980), who mentions a sandy-muddy substrate. An extant counterpart is represented by the biostromes of *Crassostrea gigas* (Thunberg, 1793) on the tidal flats of Japan (Chinzei, 2013). Fossil *in situ C. gigas* patches described by Chinzei (2013) are strikingly similar to those of *in situ* clumps of *C. gryphoides* found in the Korneuburg Basin during road construction (own observations M.H., O.M., M.Z.).

Ostrea digitalina (Fig. 3/2): calcitic shells of broad ovoid to subcircular outline; all specimens are disarticulated. Left valves are frequently found attached to *Crassostrea* shells and are well preserved. Right valves are found floating in the sediment and range from well preserved to fragmented and abraded. Like its extant congener *Ostrea edulis*, this bivalve was most probably a sessile filter feeder in the intertidal to shallow sublittoral zone. *Ostrea* species live attached to rocks and other shells but may also settle on firm muddy sand bottoms (Stenzel, 1971). At the Stetten site, the frequent occurrence of left valves of *O. digitalina* cemented to *Crassostrea* shells clearly document that this secondary hardground was the preferred substratum.

Perna aquitanica (Fig. 3/3): aragonitic shells of elongate trigonal outline, up to 20 cm in length; all specimens are disarticulated. Most shells are complete but have been partly damaged during excavation due to the tendency of the leached shells to exfoliate into single layers. Some shells have been deposited as primary fragments, comprising only parts of the robust umbonal area; these fragments are often abraded. Extant congeners are filter feeders living in littoral and shallow sublittoral areas with nutrient-rich waters and are adapted to a wide range of salinities (Romero and Moreira, 1980). The animals are attached with the byssus to any hardground including firm mud (Vakily, 1989).

Venerupis basteroti (Fig. 3/4): aragonitic shells up to 9 cm in length; all specimens are disarticulated. The shells are well preserved. Fragmentation occurred mainly during excavation due to the fragility of the leached shells. Extant congeners of this bivalve are shallow burrowers in mixed sandy bottoms from the intertidal zone to the shallow sublittoral (Jurić, 2012; Moneva et al., 2014)

Ptychopotamides papaveraceus (Fig. 3/5): turreted aragonitic shells up to 7 cm in height; due to the dense sculpture of nodes and the adpressed whorls, the shells are quite robust and fairly well preserved. This is an extinct gastropod genus, perhaps comparable with modern *Tympanotonos* species, which live as algal feeders and detritivores in mangrove swamps and tidal flats along the coast of West Africa. The animals avoid sandy sediment (Bandel and Kowalke, 1999; Reid et al., 2008; Jamabo and Chinda, 2010). Within the succession of the Korneuburg Basin, *P. papaveraceus* forms mass occurrences in black clay deposits formed on tidal flats (Zuschin et al., 2014). Coastal mudflats were also interpreted as a habitat of this species by Latal et al. (2006) based on stable isotope signatures.

Solen marginatus (Fig. 3/6): strongly elongated, rectangular, aragonitic shells up to 18 cm in length; all specimens were found *in situ* with articulated valves. *S. marginatus* is an extant razor clam species living in sandy to muddy tidal and subtidal flats and subtidally to a few meters water depth along the European Atlantic coast, the northwest coast of Africa and the Mediterranean Sea (Milišić, 1991; Rufino et al., 2010; Hmida et al., 2010). *S. marginatus* is a filter feeder burrowing down to 60 cm deep in the sediment (Gaspar et al., 1999; Hmida et al., 2010). This species is not rare within the shell bed but could not be quantified and analyzed from DSM data because it belongs to the post-event colonizers, occurring on top of the shell bed or above: most specimens were removed during excavation without denoting their exact positions. Nevertheless, this species is of great significance for the taphonomic analysis as it is the sole bivalve species occurring *in situ* with articulated valves.

4. Methods

Terrestrial laser scanning was used to document the site as a georeferenced 3D point cloud (Otepka et al., 2013). A Faro Focus Laser scanner with a nominal point measurement accuracy of 1 mm (SD) in each coordinate and a sampling distance of approximately 1 mm was used. A total of 83 scans were made. The individual point clouds of each scan were transformed first into one common coordinate system and then georeferenced by control points to Universal Transverse Mercator (UTM) coordinates. Their precision is better than 2 mm (SD). A robust filter (pre-processing) was applied to reduce measurement noise while preserving surface structures such as sharp edges (Nothegger and Dorninger, 2009). The surface triangulation is based on the Poisson surface reconstruction method (Kazhdan et al., 2006). The points of this triangulation are the nodes for interpolating a regular grid of heights above the plane of the shell bed using the scientific software OPALS (Pfeifer et al., 2014). In addition, a Canon 60D camera with a Canon EF 20 mm f2.8 lens was used to take more than 300 photos from a moving platform. The camera was placed approximately orthogonal to the fossil bed. From the photos with a nominal ground resolution of approximately 0.6 mm per pixel, an orthophoto mosaic was generated with a resolution of 0.5 mm per pixel. The images were radiometrically corrected to enhance contrast for the visual interpretation. To detect patterns in the distribution and composition of shells, two transects (N–S, W–E) were defined, each represented by 7 tiles of 2 × 3 m length, with the central one overlapping (Fig. 4). All objects within this area were manually outlined on the digital surface model and cross checked based on the high-resolution orthophotos (Fig. 5). In total, 10.284 objects were defined and characterized in respect to taxonomy, shell position, orientation, size and fragmentation.

4.1. Taxonomy

For the data analyses, we consider only the shells of *C. gryphoides*, *P. aquitanica*, *O. digitalina*, *V. basteroti*, pectinids, and *P. papaveraceus*. This selection is based on the difficulty of identifying the usually fragmented and small shells of the other taxa from the available data set. Moreover, the aragonitic shells of the small species are slightly leached, and therefore, many specimens were damaged and/or removed during excavation, resulting in a bias by preparation. This bias is insignificant for the stable and well-preserved calcitic shells (ostreids, pectinids) and very low for the aragonitc but thick-shelled and large *Perna* and *Venerupis*. Each shell was counted as one specimen (two specimens might represent one individual in bivalves). The taxonomic category Ostreidae indet. refers to fragments which cannot be reliably identified as *Crassostrea* or *Ostrea* due to poor preservation. Most of these specimens, however, seem to be highly abraded *Crassostrea* chips.

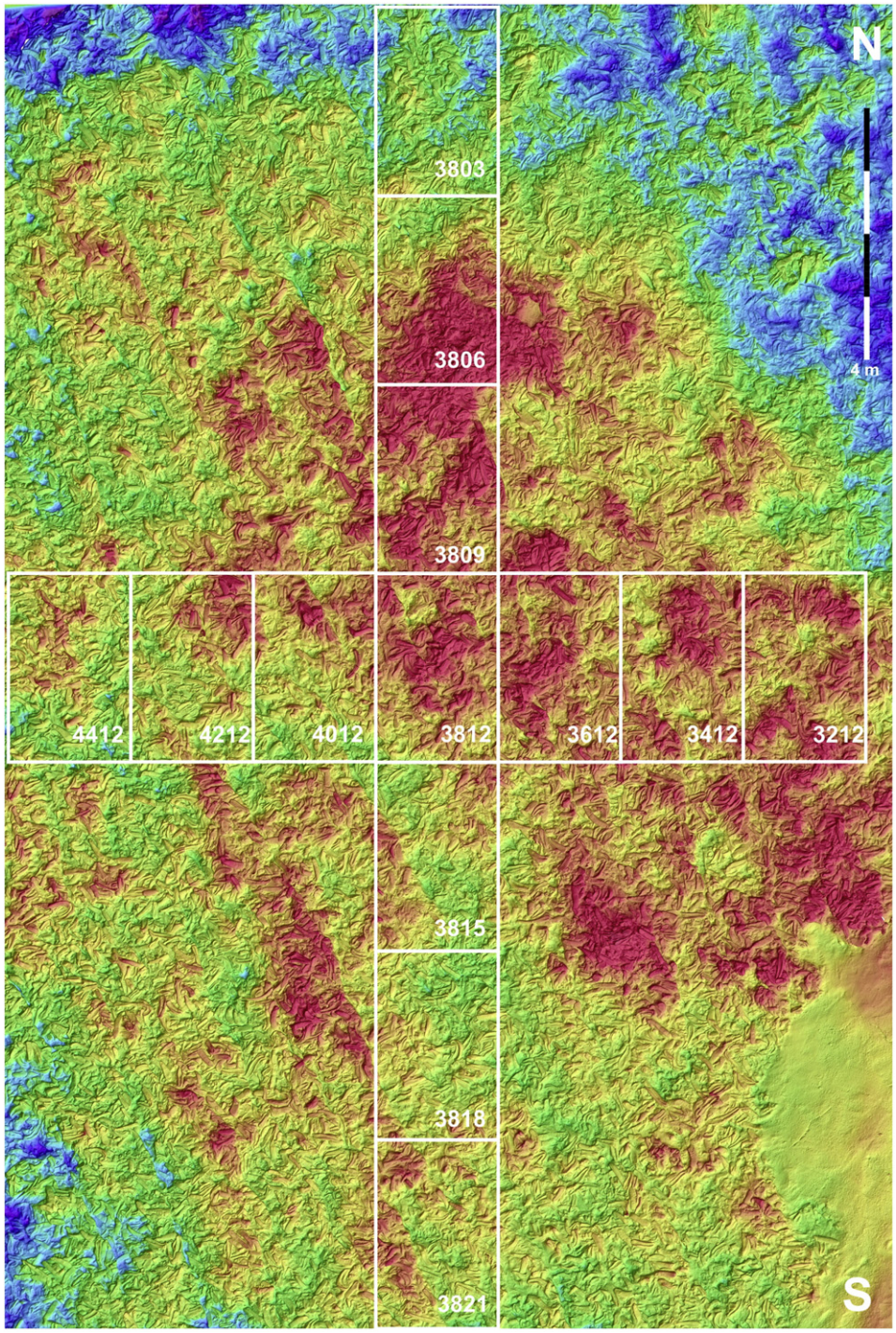

Fig. 4. Digital surface model and the position of analyzed tiles. The coloring indicates topography (red = high, blue = low). The roughly NW–SE trending fault system is a post-sedimentary structure. The current relief is thus largely tectonically induced and does not reflect an Early Miocene paleo-relief.

4.2. Convex-up/convex-down position (CU/CD) and left/right shell (CDL/CDR)

Whether the shell is a left or right valve and the convex-up/convex-down position is discussed only for *Crassostrea*. The elongate and irregular shapes of the shells clearly do not match the bowl-shaped textbook examples for such analyses (Allen, 1984; Kidwell, 1991). Nevertheless, left and right shells display considerable convexities; only the terminal parts of adult shells become rather flat. Therefore, the convex-up position of the often laterally curved shells is assumed to be very stable, requiring considerably drag forces to overturn the shells. Due to the irregular growth, the distinction between left and right shells is not possible for convex-up (CU) shells, and therefore this information is available only for convex-down (CD) shells (Fig. 5). Highly fragmented shells (e.g., shells comprising less than 1/3 of the original shell) were excluded from statistical analyses because the CU/CD attributes are of no meaning for the rather flat chips.

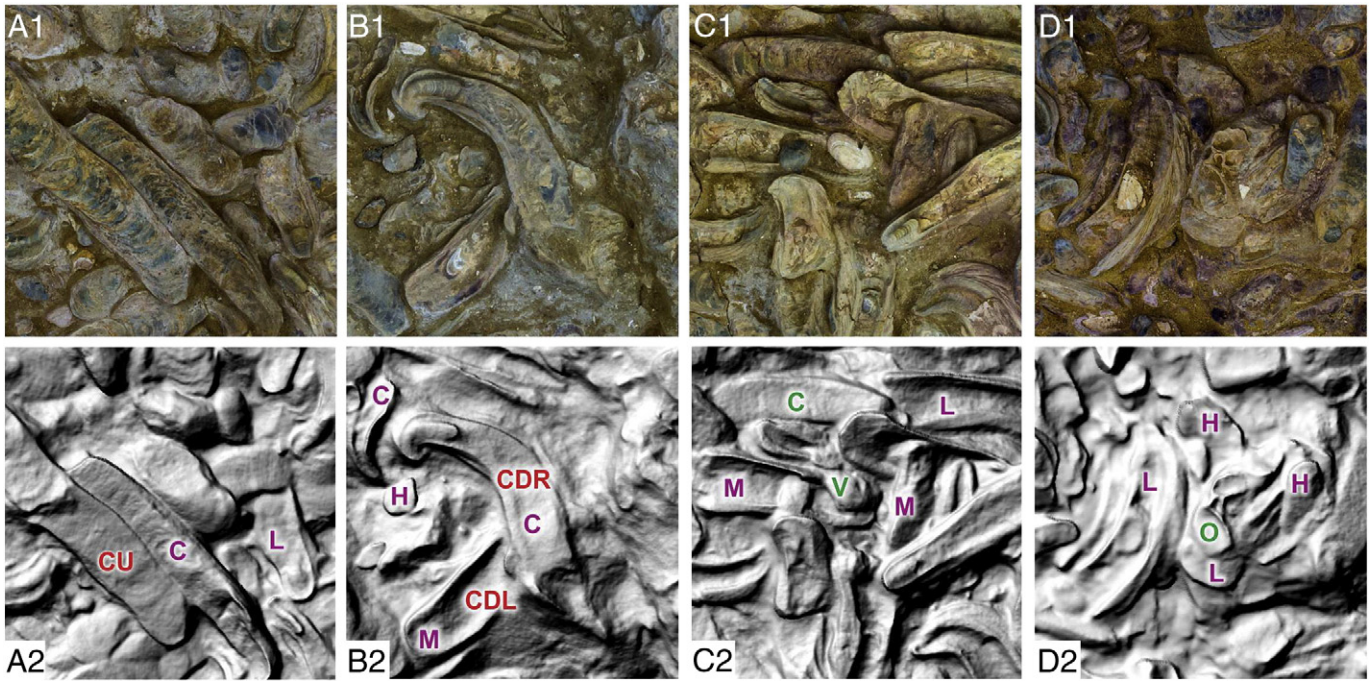

Fig. 5. Details from the shell bed: A1–D1 orthophotos, A2–D2 digital surface model (width: 0.5 m), showing alignment of shells (A1), random orientations (C1), strongly curved shells (B1) and areas with high density of fragments and attachment of *Ostrea* on *Crassostrea* (D1). Shell positions (red): CU = convex-up, CDL = convex-down left, CDR = convex-down right; fragmentation (violet): C = complete, L = low, M = moderate, H = high; taxa (green): C = *Crassostrea*, O = *Ostrea*, V = *Venerupis*.

4.3. Size and orientation

Shell length and orientation were evaluated by using their centerline, which is an imaginary curved line spanning the maximum length of the shell. For the automatic determination of the centerline, we used the shell margins, which comprise about 1000 points on average. For each shell, this outline point number was reduced to 100 and then filtered to points with close to even spacing. In a next step, a Delaunay triangulation was calculated between the filtered outline points (Delaunay, 1934), constrained by the edges between the outline points. To find the centerline for each oyster outline, the Voronoi diagram was formed (Voronoi, 1908) from the triangulation. The edges between neighboring Voronoi vertices within the boundary are the medial axis transform (MAT) for the oyster outline (Aichholzer et al., 1996). The longest path in this tree was found using Dijkstra's algorithm between MAT end points (Kirk, 2015).

Shell orientation was automatically deduced from the centerlines as well. No experimental data on the hydrodynamic behavior of the very irregularly shaped *Crassostrea* shells are available. Therefore, the U- and S-shaped shells were excluded from analysis and only more or less straight and elongate shells with a centerline length of ≥18 cm were analyzed; fragments were excluded. Strongly curved shells were defined as objects in which the vertices of the centerline form angles >205° or <155°. This yields a considerably reduced data set of only 529 shells for all tiles. No difference between the anterior and posterior part of the shells was made. Therefore, the measured angles range from 0° to 180°; for visualization, the rose diagrams (Fig. 6) are mirrored.

4.4. Degree of fragmentation (only for Crassostrea)

Four categories of fragmentation were used (Fig. 5): *complete* shells are fully preserved or display only minor damage, which might have

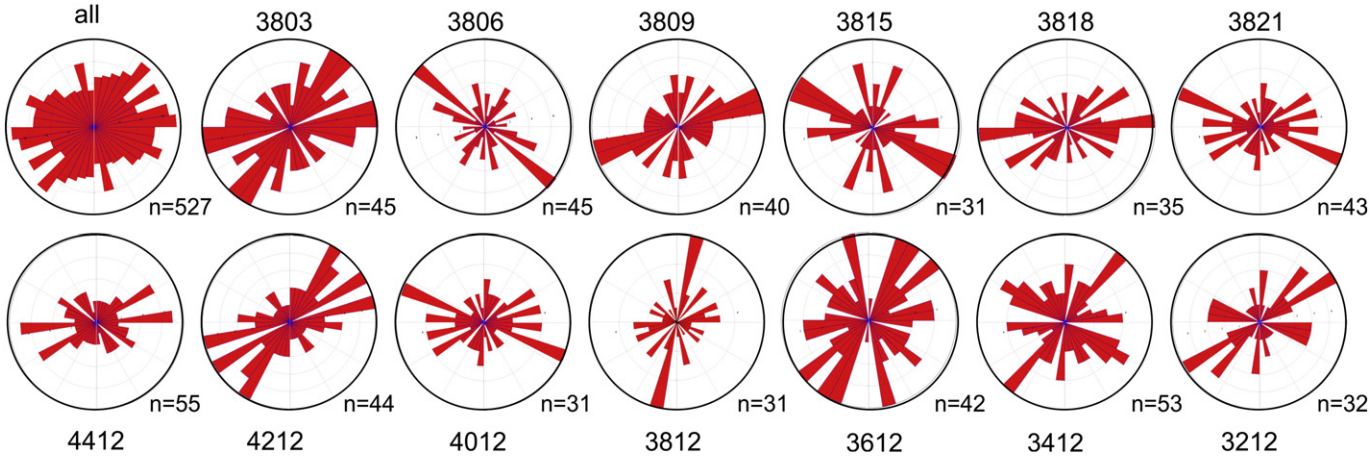

Fig. 6. Rose diagrams showing the orientations of *Crassostrea* shells per tile (red). Note that the 0–180° data are mirrored for visualization.

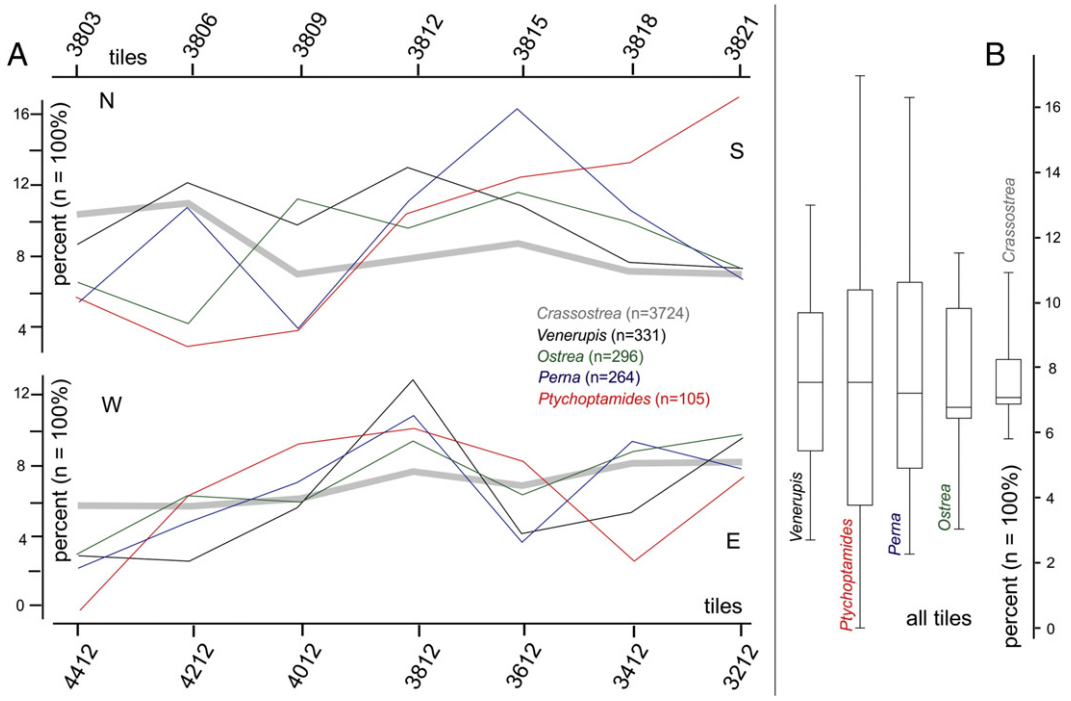

Fig. 7. Quantitative data of five species derived from the digital surface model. (A) Counts of specimens per taxon in percentages per tile revealing distinct differences in spatial distribution. (B) Boxplots including data of all tiles visualize this pattern, indicating the comparatively lowest interquartile range for *Crassostrea*.

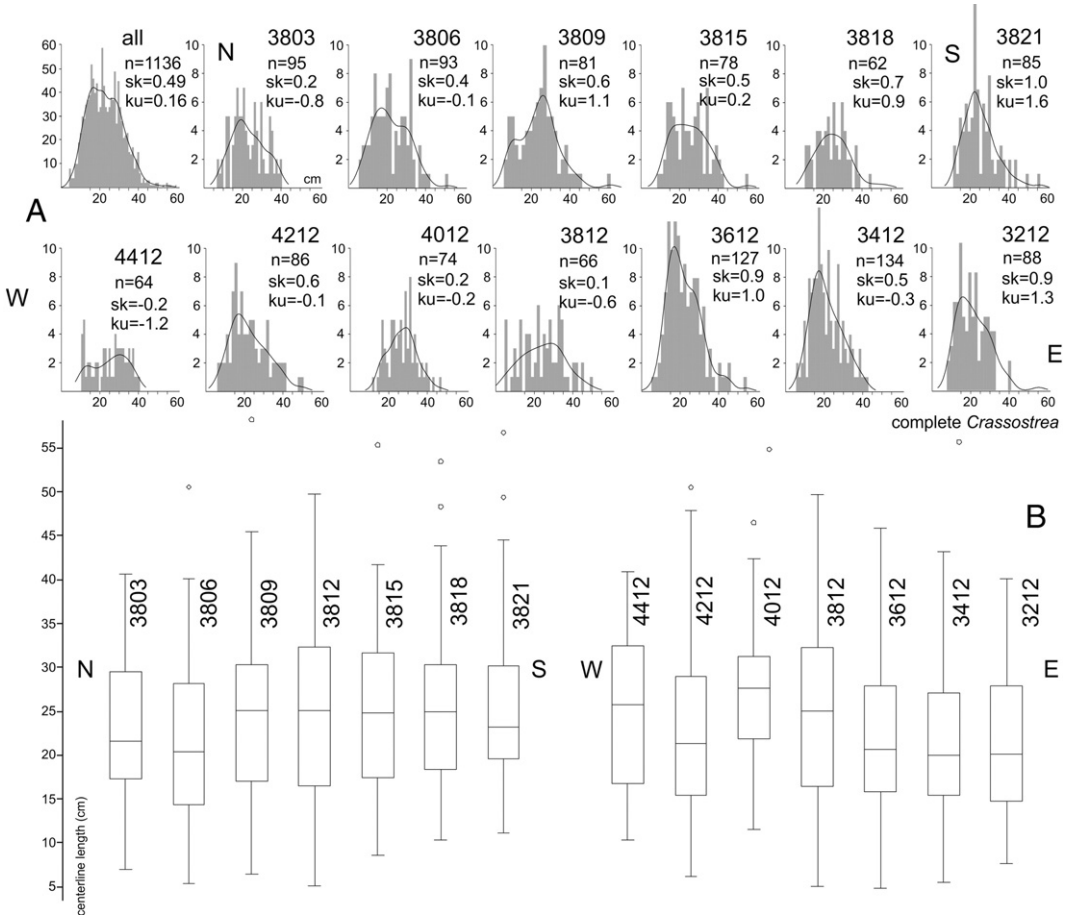

Fig. 8. Size–frequency distribution diagrams and boxplots of the same data for complete *Crassostrea* shells per tile (based on centerline lengths). A near normal distribution with slightly positive skewness reflects the original size classes in the oyster biostrome. No significant N–S or W–E trends are recognizable.

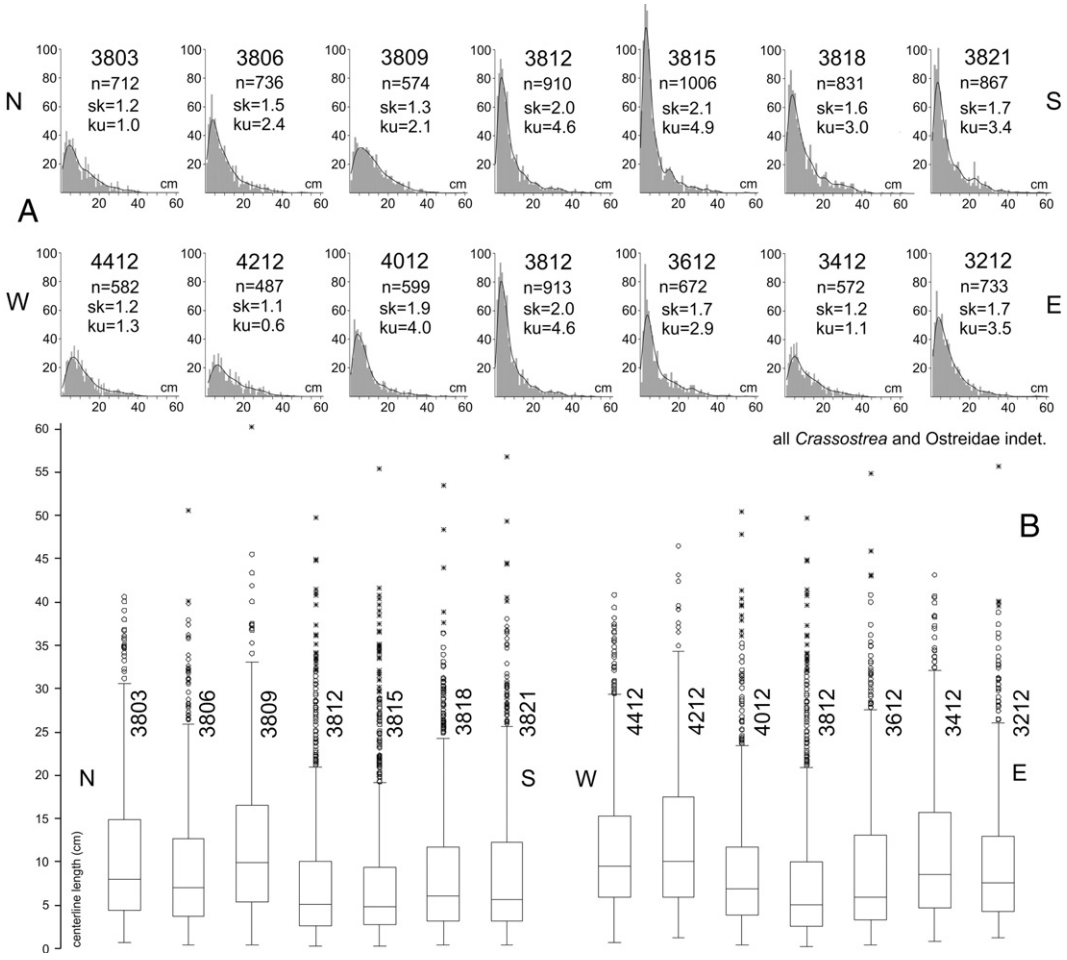

Fig. 9. Size–frequency distribution diagrams and boxplots of central-line lengths of all objects identified as *Crassostrea* and Ostreidae indet. including highly fragmented shells. Fragments <5 cm predominate all spectra but are most prominent in the southern tiles.

occurred already during the life of the animal ($n = 1121$). The category *low fragmentation* comprises shells in which not more than ¼ of the assumed length is missing ($n = 951$). *Moderate fragmentation* is defined by representing at least ½ of the original shell lengths ($n = 1638$). The category *high fragmentation* comprises 4458 specimens of strongly damaged shells representing less than ¼ of the complete shell. Note that the attribute fragmentation does not contain any information on abrasion.

All of this information was analyzed in respect to the entire area and for each individual tile. The data were stored in a georeferenced ArcGIS database and are available online in Table 2 (supplementary data).

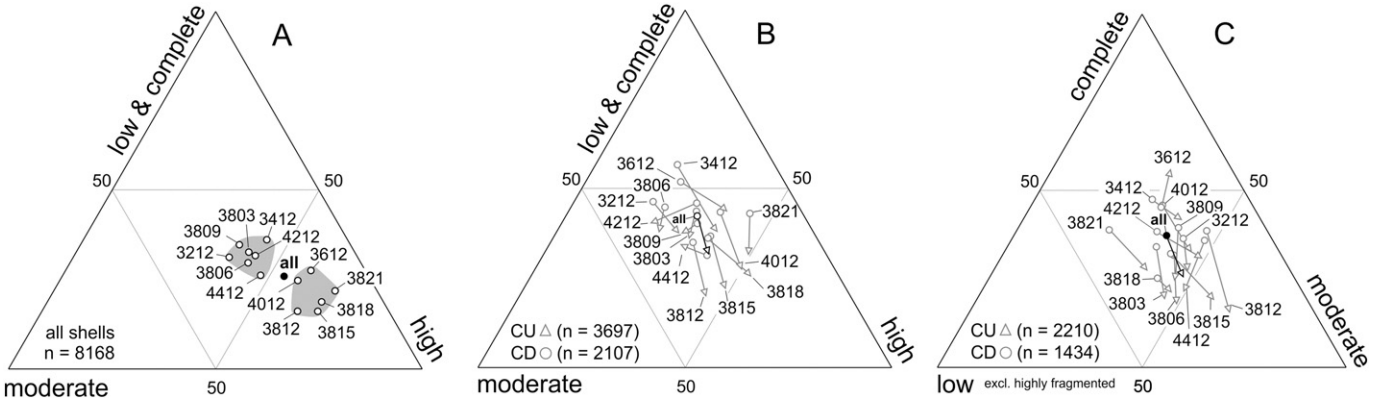

Fig. 10. Ternary diagrams documenting the predominant taphonomic grades per tile (A). The same data set reduced to shells identified as convex-up (CU) or convex-down (CD) (B) and after removal of highly fragmented specimens (C), both showing lower taphonomic grades of CU shells.

5. Results

5.1. Composition of the shell bed

The shell bed is a single, about 15- to 25-cm-thick horizon intercalated in coarse, poorly sorted sand with scattered plant debris and mudclasts. The inventory in all tiles is predominated by disarticulated *Crassostrea* shells, which represent 8168 individuals out of 10,284 objects. The remaining objects comprise 331 *Venerupis*, 296 *Ostrea*, 264 *Perna*, 105 *Ptychopotamides* and 7 pectinids. In addition, 1113 shells were treated as Ostreidae indet. and are highly abraded shell chips. Despite the homogeneous impression at first sight, the distribution and number of *Crassostrea* shells fluctuates. Within the 13 tiles, the number of *Crassostrea* shells ranges from 385 to 974 specimens with a mean of 628 ($\sigma = 171$). These include strongly fragmented but identifiable shells. Removing these fragments results in a more balanced pattern of 219 to 402 shells per tile with a mean of 285 ($\sigma = 54$). Overall, the trend in shell density increases in the S–N and W–E directions.

The distribution of the other taxa is also inhomogeneous. For a better visualization, the total number of specimens per taxon was transformed to percentages and calculated per tile (Fig. 7A). While *Crassostrea* shows a comparatively low variation, all other taxa have significant high (e.g., tile 3812) and low values (e.g., tile 4412). A significant correlation of occurrences of *Venerupis*/*Crassostrea* ($r = 0.67$, $p = 0.01$) and of *Venerupis*/*Perna* ($r = 0.63$, $p = 0.02$) was evident. No correlation at all exists for *Ostrea*/*Crassostrea* or for *Ptychopotamides* in general. Box plots of the distributional data (%) for all tiles (Fig. 7B) reflect these patterns as well and show low variation for *Crassostrea* and comparatively wide interquartile ranges for all other taxa.

5.2. Size distribution of Crassostrea shells

A total of 1,121 complete *Crassostrea* shells are recognized, with the largest specimen attaining 60.1 cm in length. The mean central-line length is 23.7 cm ($\sigma = 9$ cm); the interquartile range is approximately 17–30 cm. The size–frequency distribution has a moderately positive skewness (0.49) and low kurtosis (0.16), indicating a near normal distribution (Fig. 8). Using the central-line length of all objects identified as *Crassostrea* and Ostreidae indet. (including the highly fragmented shells) yields a completely different pattern. The main components of the shell bed are fragments. Consequently, the size–frequency distribution has a strongly positive skew in all tiles (Fig. 9). In total numbers, small fragments (<50 mm) are most frequent in southern and eastern tiles. This N–S trend correlates also with an overall increase in kurtosis.

5.3. Taphonomy of Crassostrea shells

The initial impression is that of masses of perfectly preserved shells. A closer look, however, reveals a more complex pattern. Overall, only 25% of the shells display no (1121 shells) or only low (951 shells) damage and fragmentation. Another 20% are moderately well preserved (1638 shells), and the majority (55%) comprise highly fragmented specimens (4458 shells). In ternary diagrams, the predominant taphonomic grades per tile form two distinct clusters, which are also supported by the cluster analysis (not shown). Northern (3803, 3806, 3909), western (4412, 4212) and eastern (3412, 3212) tiles tend to have lower contributions of highly fragmented shells, while the central and southern tiles (4012, 3812, 3212, 3815, 3818, 3821) are characterized by high numbers of fragments (Fig. 10A). This pattern remains stable even if only those valves are considered which also can be reliably identified as convex-up (CU) or convex-down (CD) (Fig. 10B). Interestingly, in nearly all tiles the CU shells have lower taphonomic grades than the CD shells. Even when excluding the highly fragmented and usually flat shells, the different taphonomic grades between CU and CD shells remain significant (Fig. 10C).

5.4. Convex-up/convex-down and left/right relations of Crassostrea shells

Clearly, a significant negative correlation occurs between CD and CU shells ($r = -0.92$, $p = 0.0001$), but more interestingly, the convex-up position predominates in most areas. Especially along the N–S transect, CU shells occur up to twice as often as the CD shells (with a slight decreasing trend). Within the W–E transect, tiles 4412 and 4212 are balanced and also the easternmost tiles 3612–3212 have nearly balanced CU/CD ratios. Only the CD shells expose hinge and muscle scar and therefore can be separated into left (CDL) and right (CDR) valves. Overall, the ratio is nearly balanced as 39.5% of all CD shells are left ones and 40.7% are right shells; 19.8% remain undefined due to cover by sediment or other shells. The mean CDR/CDL ratio of the defined shells is 0.97 ($\sigma = 0.2$), and the moderate correlation in Fig. 11A ($r = 0.49$) mainly reflects the fluctuating amount of undefined shells per tile. A further highly significant correlation is observed for the CU/CD ratio and the number of specimens ($r = 0.85$, $p = 0.0002$) (Fig. 11B) if the outlier tile 4012 is excluded. Thus, low densities such as observed in the westernmost tiles 4412 and 4212 correlate with equal CU and CP positions, while high-density areas, such as the northernmost tiles 3803 and 3806, are characterized by predominant CU positions. Only tile 4012 is a clear outlier with a CU/CD ratio of 2.3 and a moderate density of only 229 shells.

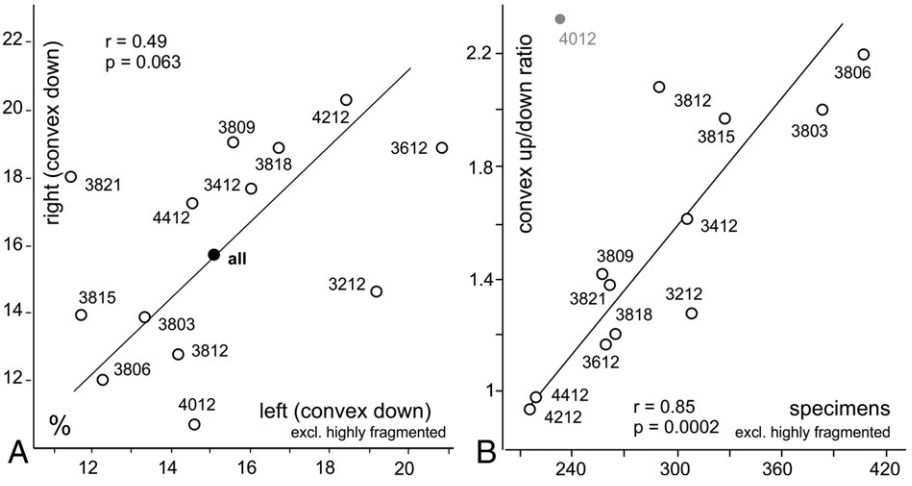

Fig. 11. Correlations between right and left shells (only for CD shells) (A) and between CU/CD ratio and the number of specimens per tile (B).

5.5. Orientation of shells

The elongate and large shells of *Crassostrea* are expected to be excellent indicators of predominant hydrodynamic currents. Nevertheless, the data of all tiles do not indicate any significantly preferred direction aside from a very weak W–E preponderance. The low number of suitable shells per tile is problematic for the analysis of individual tiles (Fig. 6). Therefore, the tiles were grouped according to geographic position. This grouping reveals a quite inhomogeneous pattern (Fig. 6). A very clear NE–SW alignment characterizes the eastern tiles. Similarly, a distinct W–E orientation is evident in the south. This main orientation also occurs in the western sector but the variation is larger. In the north, however, the shells are randomly oriented.

6. Discussion

The shell bed is an exceptional structure in the Miocene basin fill of the Korneuburg Basin. No comparable shell bed was detected by Zuschin et al. (2014) within the 445-m-thick sedimentary succession underlying the Stetten site. Historical data of the clay pit area suggest a much wider lateral distribution of the shell bed across an area of at least 10,000 m^2. Throughout its distribution area, it has a sheet-like appearance with about 15–25 cm thickness and sharply overlays a unit of fossil-poor coarse sand lacking any oyster shells. Not a single articulated specimen was ever found in this characteristic horizon, which was well known to the miners and collectors. Therefore, our main hypothesis is that most of the shell bed represents an event bed sensu Einsele et al. (1991) and Kidwell (1991), which amalgamated pre-event phases and was shaped by post-event processes.

6.1. Paleoecological data—fits and misfits

The different ecological requirements of the species clearly suggest mixing of different habitats, which might have been spatially and/or chronologically separated. The first recognizable phase is that of the flourishing oyster biostrome. Extant *Crassostrea* biostromes are generally characterized by rather low molluscan diversity. Stiner (2006) detected 19 mobile species of shelled molluscs in the *Crassostrea virginica* biostrome of Mosquito Lagoon in Florida, and Boudreaux (2005) encountered 10 (semi)-sessile species within the same ecosystem (Boudreaux et al., 2006). Harwell (2010) and Harwell et al. (2010) encountered 22 molluscan species in the *C. virginica* and *C. ariakensis* biostromes in the Chesapeake Bay region in Maryland, and Quan et al. (2009) collected 11 mobile epibenthic species from a *Crassostrea rivularis* biostrome in the Yangtze River estuary in China. A comparison of these lists with those obtained from the Stetten site documents parallels on the generic level (*Nerita*, *Nassarius*, and *Polinices*) and on the family level (e.g., calyptraeids, muricids, and mytilids). Many other taxa of the death assemblage associated with the shell bed most probably did not live in the intertidal zone within the secondary hardgrounds provided by living and dead *Crassostrea* shells. This is clearly the case for the pelagic nautilid *Aturia aturi* but also for the pectinids and the large and burrowing razor clam *S. marginatus*. Similarly, the shallow-burrowing *V. basteroti* was certainly not part of the intertidal *Crassostrea*–hardground ecosystem. Nevertheless, the shells could have been washed ashore from adjacent sandy shores and admixed to the oyster shells. The lack of abrasion and the very low grade of observed fragmentation (if not entirely due to inadequate preparation), however, do not hint at a longer residence and movement between the "rocky" *Crassostrea* shells. Some transport, however, is evident from the complete disarticulation. Moreover, the shells are found roughly parallel to the bedding plane and not in chaotic positions. The significant correlation of *Venerupis* and *Crassostrea* occurrences suggests that both taxa had passed through the same taphonomic process. Therefore, we suggest that *Venerupis* had settled foreshore sand that had already covered the oyster biostrome. Thus, *Venerupis* is a representative of a chronologically second phase amalgamated in the shell bed. Given the very high sedimentation rates in the basin of approximately 60–100 cm/1000 years (Zuschin et al., 2014), this second phase might represent only a few hundred years. Subsequently, during a high-energy event, both the *Crassostrea* biostrome and the infaunal fauna of the overlying sand became reworked and mixed, forming an event deposit *sensu* Einsele et al. (1991) and Kidwell (1991). The rare shells of the pelagic cephalopod *Aturia* might have been transported into the estuary during this event as well. Most of the *Perna* shells seem to have accumulated also during this second phase, and therefore, *Perna* is significantly correlated with *Venerupis* but less so with *Crassostrea*. Phases 1 and 2 can thus be classified as pre-event stages of local depositional systems.

The occurrence of *Ostrea* is not correlated with any other taxon. The shells are largely attached to *Crassostrea*, often settling on the interior part of convex-down shells. They represent the third phase and the first stage after the catastrophic event. *Crassostrea* shells now formed secondary hardgrounds in the shallow estuary. Patchiness of *Ostrea* occurrences may at least partly be explained by the presence of "shell-islands" on a seafloor, which slowly became covered by sand again. Of course, we cannot exclude that some *Ostrea* settled shells already during phase 1. An alternative scenario is that *Ostrea* started to settle during a phase of higher salinity. Such a shift in faunal composition was documented by Parker (1955) for recent oyster biostromes in Texas, where *Crassostrea* was outcompeted by *Ostrea* during a phase of increased salinity. The absence of other high salinity indicators, such as echinoderms and strombid and cassiid gastropods, however, does not support this hypothesis. In any case, the frequent occurrence on the inner surface of *Crassostrea* shells indicates that *Ostrea* settlement took place after the death of the *Crassostrea* specimens.

Similarly, the mudflat-inhabiting gastropod *P. papaveraceus* is an unlikely member of the *Crassostrea* biostrome ecosystem. Again, this species could have been washed-in from adjacent mudflats, but this hypothesis is in conflict with the absence or rareness of other mud whelks, such as *Granulolabium* and *Terebralia*, which are otherwise very abundant within the Stetten section (see Zuschin et al., 2014) and usually associated with *Ptychopotamides*. Therefore, its frequency points to a selective mechanism introducing *Ptychopotamides* into the area. A possible mechanism would be hermit crabs, which are well known to occupy potamidid shells (Wells, 2003; Willan, 2013), resulting in out-of-habitat transport (Houbrick, 1992). The distribution pattern of *P. papaveraceus* does not correlate to those of *Crassostrea*, *Perna* and *Venerupis*, supporting the hypothesis that this snail's distribution reflects a post-event situation. In particular, the N–S trend in frequency could indicate a topographic and/or environmental gradient in the estuary.

The *in situ* occurrence of *Solen* and the fact that it is the only species found with articulated valves clearly indicate that it settled the area after the formation of the shell bed. The position within the *Crassostrea* shells suggests that the shell bed acted as physical barrier for the deep-burrowing razor clams, comparable to the "forced within-habitat concentration" defined by Mandic et al. (2004b). The lack of *in situ* specimens of other bivalves, such as shallow-burrowing venerids and cardiids, shows that several tens of centimeters of sediment had already accumulated above the shell bed and only deeply burrowing taxa could reach the shell bed. Thus, the solenids witness a fourth phase of settlement, amalgamated in the shell bed.

6.2. Patterns

The shell bed is a distinct horizon within coarse sand, lacking any coarsening/fining-upward trends toward over- and underlying units. All shells except *Solen* are disarticulated and the vast majority of shells are found more or less parallel to the bedding plane, except for oblique positions resulting from leaning on other shells. Therefore, as discussed above, the main part of the shell bed is interpreted as an event layer

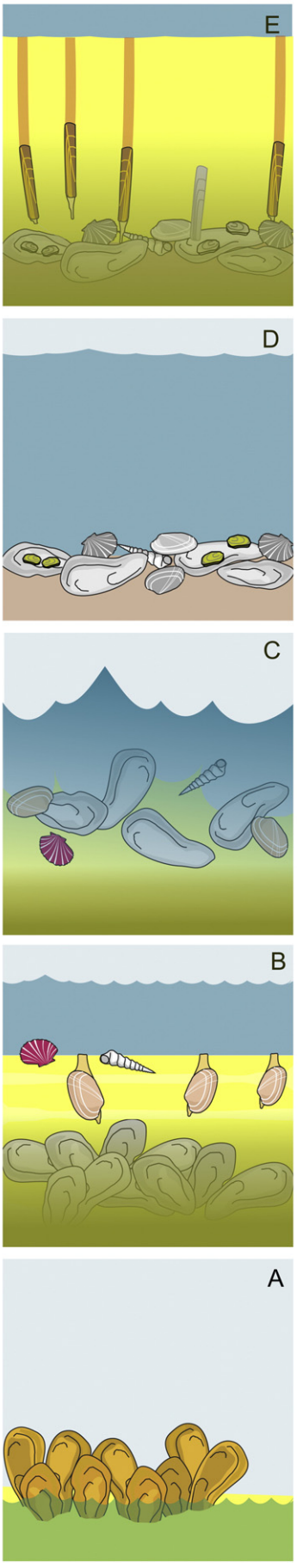

amalgamating two chronologically successive phases (phase 1: *Crassostrea* biostrome; phase 2: foreshore sand flat with *Venerupis*). As chaotic orientations within the sediment are absent, a mass transport as debris flow can clearly be excluded. Hence, we hypothesize that after the high-energy event, the shells have been part of the sea bottom for a certain period and were exposed to water energy (phase 3: secondary hardground with *Ostrea* settlement). The near normal distribution in size–frequency distribution, with most *Crassostrea* shells ranging from 17 to 30 cm and very large shells merely forming outliers, is interpreted to reflect the natural size distribution of the mature, living oyster biostrome of phase 1. For bivalves living in the intertidal zone, vertical growth is limited, and larvae have little possibility to settle in the densely packed structure (Strayer et al., 1996). This might partly explain the low contribution by small and subadult shells. In addition, small shells will be underrepresented due to strong predatory pressure (e.g., Kulp et al., 2011; Carroll et al., 2015). Similarly, the rareness of very large and old shells is a function of the declining survival rate with ontogenetic age. Thus, although the oyster biostrome is clearly not *in situ* but reworked, the original community structure still seems to be reflected. Lack of sorting caused the accumulation of very small or very large shells. Similarly, the equal contribution by left and right valves points to the preservation of the primary composition and contradicts the hypothesis of hydrodynamic sorting and selective transport.

The distribution of fragmentation, in contrast, is less homogeneous, and the grouping of southern and central tiles with high contributions of fragmented *Crassostrea* shells (versus fewer fragments in the north, west and east) might reflect different environmental settings. This also fits the observed trend of increasing shell density in S–N and W–E directions. Traditionally, the interpretation of the significant dominance of convex-up positions in most tiles would be that water energy was high enough to favor the preservation in this stable position (Kidwell and Bosence, 1991). In addition, the stable convex-up position increases significantly with shell density. This may indicate that high water energy led to a denser accumulation and simultaneously turned over convex-down shells into the stable position. Moreover, the fragmented specimens were comparatively lightweight and morphologically less complex than the complete shells. Therefore, less energy was necessary to force them in the stable convex-up position. This would explain the offset between convex-down and convex-up shells shown in Fig. 10. The presence of such water energy involving waves or currents should also be traceable in shell orientations. These orientations, however, are quite inhomogeneous across the shell bed, ranging from random in the north, to NE–SW oriented in the east, and W–E oriented in the south. None of the analyzed features correlates convincingly with the prevailing orientation pattern. For example, high CU/CD ratios, which might point to high water energy, are not correlated with dominant orientations and vice versa. Examining the seemingly significant prevailing orientations in single tiles reveals contradicting patterns in adjoined tiles. Specifically, a distinct NW–SE direction in tile 4012 is opposed by SW–NE directions in the neighboring tiles 4212 and 3812. These contradictions cast doubt on the significance of the orientations, and we propose two hypotheses to interpret the patterns:

1. The high-energy event, which reworked the oyster biostrome and homogenized it across the now visible area, will most probably have had a directional component, such as the run-up and backwash of a tsunami. The observed settlement by epibionts and bioerosion could have occurred already while the animals were alive. In many cases, however, the epibionts are attached only to the internal

Fig. 12. Cartoon showing the hypothetical steps of shell bed formation: (A) Intertidal *Crassostrea* biostrome. (B) Died-off biostrome covered by foreshore sand with shallow-burrowing bivalves and pectinids. (C) Exhumation of the oyster shells and amalgamation with the infauna from overlying sand during a tsunami or heavy storm. (D) Secondary hardground on the sea floor below fair weather base. *Ostrea* starts to settle on the empty shells. (E) Rapid burial by sand and settlement by deep-burrowing solenoid bivalves.

surfaces of *Crassostrea*, clearly indicating a post-mortem settlement. *Crassostrea* shell half-lives are very short, ranging from a few years to few decades (Powell et al., 2006, 2012; Waldbusser et al., 2011). Therefore, the shells were apparently exposed on the sea bottom for at least some time. During this phase, the original orientation will have been strongly biased by bioturbation and the dominant hydrodynamic setting. In particular, bioturbation by large marine vertebrates such as rays, turtles and teleost fishes is a common phenomenon in shallow marine settings (Kidwell and Bosence, 1991; Gregory, 1991; Pearson et al., 2007; Lazar et al., 2011; Pervesler et al., 2011). The vague NE–SW pattern in many tiles may thus be a strongly distorted echo of the original tsunami or storm-wave signature. In addition, we cannot rule out that overlapping storm waves modified the orientations.

2. A closer examination reveals that "significant" directions are often forced by groups of densely aligned shells. Due to the density, shells might simply become jammed in a certain position by bioturbation or an occasional agitation by waves. The jammed shell will clearly have the same orientation as its neighbor due to the straight and elongate shape. In addition, some of the irregularly shaped shells might have acted as stable anchors, which blocked rotation in current direction. Accepting this hypothesis leads to the conclusion that the clusters of oysters with similar orientation do not necessarily indicate any prevailing and persistent current. The forces in the strongly wave-exposed upper shore face, however, would have overcome the blocking and jamming effects and would surely have resulted in a uni- or bimodal distribution. Therefore, the shell bed was below fair weather base or was in a protected position within the estuary.

Similarly, the partly high CU/CD ratio is not necessarily related to constant water energy or a certain current regime but may be a "maturity" effect. During the years of exposure on the sea floor, shells eventually became turned over by occasional high-energy events or bioturbation and remained in the stable position. Strongly curved and jammed CD shells remained unaffected. Moreover, very slender, flat and elongate shells (especially right valves with protruding hinge) will not be much more stable in the convex-up position.

This "maturity" effect, however, does not explain the opposing trends of S–N increasing shell density and S–N decreasing fragmentation and fragment frequency. No shift toward smaller shells is seen in complete *Crassostrea* in the southern tiles (Fig. 8). Therefore, a post-event sorting of fragments during phase 3, when the shell bed was exposed on the seafloor, can be excluded. The pattern may thus be the "echo" of the original distribution during phase 1, when the biostrome flourished.

6.3. Tsunamite or tempestite?

The shell bed is an event deposit resulting from a high-energy process of short duration, such as a strong storm or a tsunami. Thus, the shell bed might represent parts of a tempestite or a tsunamite. Indeed, tsunamis are very frequent events on a geological scale. About 500,000 tsunamis may be expected globally per 1 million years based on calculations of Scheffers and Kelletat (2003). Moreover, earthquakes as a trigger of a high-energy hydrodynamic event are likely to have occurred frequently during the late Early Miocene in this seismically active area. At that time, the Korneuburg Basin started to form as a junction between Alpine and Carpathian mountain chains, and the adjacent Vienna Basin also experienced a major phase of tectonic reorganization (Kováč et al., 2004; Hölzel et al., 2010; Dellmour and Harzhauser, 2012). The differentiation between tsunami-generated deposits and storm deposits, however, is difficult. Nearly all sedimentary signatures reported in the literature to characterize tsunami-generated deposits are opposed by contradicting cases casting doubt on simple models (see Morton et al., 2007; Engel and Brückner, 2011; Goff et al., 2012 and Shanmugam, 2012, for extensive reviews and examples).

Tsunami deposits form as a product of tsunami run-up or backwash and may be deposited onshore or offshore (Bahlburg et al., 2010). The conceptual models for tsunami-related deposition define an initial triggering stage (usually by earthquakes, volcanic eruptions and landslides), a tsunami stage (in which energy travels through the water without transport of water), a transformation stage (when the tsunami wave approaches the coast and incorporates sediment) and a depositional stage (with sediment deposition onshore and additional marine debris flows and turbidity currents triggered by the return flow) (Shanmugam, 2006). This model strongly focuses on the bypass function of outgoing sediment flows, settling their load in deepwater environments. Studies on coastal tsunami versus storm deposits of Bourgeois (2009) suggest that wedge-like bed-load dominated deposits are more typical for storms, whereas sheet-like, suspended-load dominated deposits point to tsunamis. Morton et al. (2007) document that sandy tsunamites are generally <25 cm thick, extend hundreds of meters inland from the beach and comprise a single homogeneous bed that is normally graded overall and typically contains mud intraclasts. Sandy storm deposits tend to be >30 cm thick, are composed of numerous subhorizontal planar laminae that are normally or inversely graded and lack internal mud laminae and rarely contain mud intraclasts. The sedimentology of the oyster shell bed fulfils some of these requirements for a tsunamite, such as sheet-like appearance, low thickness and presence of mudclasts. The overall setting, however, contradicts an onshore formation but suggests a shallow submarine depositional setting represented by phases 2 and 3 of our model. The occurrence of the pelagic cephalopod *Aturia* further indicates input of open marine waters into the protected estuary. As a detailed sedimentological analysis of the section is beyond the scope of this study, the question if the shell bed is a tsunamite or a tempestite remains unanswered, although some lines of argument tend toward a tsunamite.

7. Conclusions

High-resolution terrestrial laser scanning coupled with orthophotos are a major step forward in analyzing large paleontological data sets in a spatial and taphonomic context. The georeferenced data set enables a continuous data control and facilitates the handling of thousands of individual objects. Simultaneously, the objectivity in measurements and identifications is distinctly increased and can be re-checked easily. Herein, this method, which is still rarely applied in paleontology, helped to reconstruct the depositional history of a complex, multi-phased shell bed. Based on the mean values of the analyzed tiles, about 54,000 objects are exposed in the shell bed. Of these, about 48,000 are *Crassostrea* shells. Given that the ratio between left and right valves is largely balanced, this number might reflect at least 24,000 individuals as a rough estimate. The statistical analysis contradicts the visitor's subjective impression that large and complete shells dominate and emphasizes the high contribution of fragments within the structure. The discreteness of the approximately 15- to 25-cm-thick shell bed within comparatively fossil-poor sand, the complete disarticulation of the oysters and the horizontal position of all shells characterize the shell bed as an event layer. Moreover, the autecology of the constituents of the shell bed points to a mixing of different spatially and/or chronologically separate paleoenvironments. This qualitative approach is supported by quantitative analysis and especially by the correlations and non-correlations in density and occurrence between the various species.

Most of the *Crassostrea* shells are interpreted to derive from an initial oyster biostrome that flourished in the shallow estuary (Fig. 12). This biostrome was most probably structured into clumps. Comparable patches of *in situ Crassostrea* clumps are exposed within the geopark and were detected during road construction close to the site. A near normal distribution of shell sizes and the balanced ratio between left and right valves still reflects the original age structure of the oyster biostrome.

Unsurprisingly in such a mobile environment, the oyster biostrome soon became covered by sediment and died-off. Foreshore sand flats established, in which shallow-burrowing bivalves dwelled (Fig. 12). This development was interrupted by a massive high-energy event that reworked the oyster shells and the overlying sand with its fauna and amalgamated and homogenized the shells. This explains the significant correlation of the ecologically contradictory *Crassostrea* and *Venerupis*. The spatial variability of the biostrome was largely lost. Based on the present data, this event cannot be clearly associated with a tsunami or an exceptional storm. In respect to the setting in a tectonically highly active region, a seismically triggered tsunami wave would at least not be unlikely. Subsequently, the shell bed formed a secondary hardground for a few years (Fig. 12). *Ostrea* and balanids attached to the *Crassostrea* shells and are abundant in the interior part of convex-down shells. Although the high-energy event might be expected to have had a directional force, no distinct main orientation pattern is preserved in the shell bed. Most of the analyzed 6 m^2 tiles suggest significant orientations of the shells, which often are in conflict with predominant orientations in neighboring tiles. We hypothesize that such patterns result from "forced alignments" of elongate shells due to their spatial density, occasional movement by waves or currents, and due to bioturbation by vertebrates. Anchoring of irregularly shaped shells and subsequent leaning will produce local shell groups of similar orientation despite a position below the wave and current-agitated zone. Similarly, the patchiness of convex-up/convex-down positions with the overall dominance of CU shells is a function of "time-averaging" leading to an accumulation of stable positions rather than being related to a single event and flow regime. Finally, the shell bed became sealed by sand again rather quickly. No shallow-burrowing species are documented *in situ* from that phase. Instead, only the deeply burrowing *Solen* became stuck in the shell bed and are still preserved in life position with articulated valves (Fig. 12).

Thus, we clearly document that caution is necessary when interpreting shell beds in a geological context. In particular, the attempt to use shell beds as indicators for tsunamites may be difficult due to severe post-event modifications of the primary patterns. Similarly, reconstructions of paleo-currents based on single-area data sets are very dangerous.

Supplementary data to this article can be found online at http://dx.doi.org/10.1016/j.palaeo.2015.07.038.

Acknowledgments

Many thanks go to Josef Piller and Irene Faissner from the "Fossilienwelt Weinviertel" for their support during the laser scanning campaign. We are grateful to Sharif Hasan and to Francisco Arroyo Pinilla for their help in data acquisition (supported by the EU Program *Leonardo da Vinci*). Two anonymous reviewers greatly improved an earlier version of this paper. The study was financed by the Austrian Science Fund (FWF project no. P 25883-29 "Smart-Geology für das größte fossile Austernriff der Welt").

References

Aichholzer, O., Aurenhammer, F., Alberts, D., Gärtner, B., 1996. A novel type of skeleton for polygons. Springer, Berlin, Heidelberg, pp. 752–761.
Allen, J.R.L., 1984. Experiments on the settling, overturning and entrainment of bivalve shells and related models. Sedimentology 31, 227–250.
Bahlburg, H., Spiske, M., Weiss, R., 2010. Discussion of "Sedimentary features of tsunami backwash deposits in a shallow marine Miocene setting, Mejillones Peninsula, northern Chile, Sedimentary Geology, 178(3/4), 259-273" by Cantalamessa and Di Celma (2005). Sediment. Geol. 228, 77–80.
Bandel, K., Kowalke, T., 1999. Gastropod fauna of the Cameroonian coasts. Helgol. Mar. Res. 53, 129–140.
Beer-Bistrický, E., 1958. Die miozänen Buccinidae und Nassariidae des Wiener Beckens und Niederösterreichs. Mitt. Geol. Ges. Wien. 49 (1956), 41–84.
Boudreaux, M.L., 2005. Native and invasive sessile competitors of the eastern oyster *Crassostrea virginica* in Mosquito Lagoon, Florida (M.S. Thesis), University of Central Florida, Orlando Florida (104 pp.).
Boudreaux, M.L., Stiner, J.L., Walters, L.J., 2006. Biodiversity of sessile and motile macrofauna on intertidal oyster reefs in Mosquito Lagoon, Florida. J. Shellfish Res. 25, 1079–1089.
Bourgeois, J., 2009. Geologic effects and records of tsunamis. In: Robinson, A.R., Bernard, E.N. (Eds.), The Sea, 15, Tsunamis. Harvard University Press, pp. 53–91.
Brocchi, G., 1814. Conchiologia fossile subapennina con osservazioni geologiche sigli Apennini e sul suolo adiacente. Tomo primo. Stamperia Real, Milano (LXXX + 56, LXXX + 240 pp.).
Brongniart, A., 1823. Mémoire sur les terrains de sédiment supérieur calcaréo-trappéen de Vicentin, et sur quelques terrains d'Italie, de France, d'Allemagne, etc., qui peuvent se rapporter a la même époque. Levrault, Paris (86 pp.).
Carroll, J.M., Marion, J.P., Finelli, C.M., 2015. A field test of the effects of mesopredators and landscape setting on juvenile oyster, *Crassostrea virginica*, consumption on intertidal reefs. Mar. Biol. 162, 993–1003.
Chinzei, K., 2013. Adaptation of oysters to life on soft substrates. Hist. Biol. 25, 223–231.
Coen, L.D., Luckenbach, M.W., 2000. Developing success criteria and goals for evaluating oyster reef restoration: ecological function or resource exploitation? Ecol. Eng. 15, 323–343.
Cossmann, M., Peyrot, A., 1919. Conchologie néogénique de l'Aquitaine. Actes de la Société Linnéenne de Bordeaux. 70, pp. 181–491.
Cuvier, G., 1795. Second mémoire sur l'organisation et les rapports des animaux à sang blanc, dans lequel on traite de la structure des mollusques et de leur division en ordre, lu à la Société d'Histoire naturelle de Paris, le 11 prairial an troisième. Magazin Encycl. J. Sci. Lett. Arts 2, 433–449.
Dall, W.H., 1895. Contributions to the Tertiary fauna of Florida, with especial reference to the Miocene silex-beds of Tampa and the Pliocene beds of the Caloosahatchie River. Part 3, A new classification of the Pelecypoda. Trans. Wagner Free Inst. Sci. Phila. 3, 483–570.
Daxner-Höck, G., 1998. Säugetiere (Mammalia) aus dem Karpat des Korneuburger Beckens. 3. Rodentia und Carnivora. Beitr. Paläontol. 23, 367–408.
de Blainville, H.M.D., 1814. Mémoire sur la classification méthodique des animaux mollusques, et établissement d'une nouvelle consideration pour y parvenir. Bull. Sci. Soc. Philomat. Paris Zool. 1814, 175–180.
de Lamarck, J.B.P.A., 1805. Suite des mémoires sur les fossiles des environs de Paris. Ann. Mus. Natl. Hist. Nat. 6, 214–221.
Basterot, B. de, 1825. Mémoire géologique sur les environs de Bordeaux. Première partie, comprenant les observations générales sur les mollusques fossiles, et la description particulière de ceux qu'on rencontre dans ce bassin (Paris (J. Tastu), 100 pp. (reprinted from Mémoires de la Société d'Histoire Naturelle de Paris 2, 1–100).
Delaunay, B., 1934. Sur la sphere vide. Otd. Mat. Estestv. Nauk 7, 793–800.
Dellmour, R., Harzhauser, M., 2012. The Iván Canyon, a large Miocene canyon in the Alpine-Carpathian Foredeep. Mar. Pet. Geol. 38, 83–94.
Deshayes, G.P., 1836. Description des Coquilles Fossiles des Environs de Paris. Deshayes, Paris, pp. 691–814.
Deshayes, G.P., 1843–1850. Traité élémentaire de conchyliologie avec les applications de cette science a la Géologie. Tome premier, Seconde Partie. Conchifères dimyaires. Masson, Paris (824 + 80 pp.).
Dubois de Montpereux, F., 1831. Conchyliologie fossile et aperçu géognostique des formations du plateau Wolhyni-Podolien. Schropp and Companie, Berlin (76 pp.).
Eichwald, E., 1830. Naturhistorische Skizze von Lithauen, Volhynien und Podolien in Geognostisch-Mineralogischer, Botanischer und Zoologischer Hinsicht. Voss, Wilna (256 pp.).
Eichwald, E., 1853. Lethaia Russica ou Paléontologie de la Russie. Schweizerbart, Stuttgart (533 pp.).
Einsele, G., Ricken, W., Seilacher, A. (Eds.), 1991. Cycles and events in stratigraphy. Springer-Verlag, Berlin (955 pp.).
Engel, M., Brückner, H., 2011. The identification of palaeo-tsunami deposits—a major challenge in coastal sedimentary research. Coastline Rep. 17, 65–80.
Férussac, A.E.J.P.J.F. d'Audebard de, 1821–1822. Tableaux systématiques des animaux mollusques classés en familles naturelles, dans lesquels on a établi la concordance de tous les systèmes; suivis d'un prodrome général pour tous les mollusques terrestres ou fluviatiles, vivants ou fossiles. Bertrand, Sowerby, Paris, Londres (XLVII + 27 + 110 pp.).
Fleming, J., 1828. A history of British animals, exhibiting the descriptive characters and systematical arrangement of genera and species of quadrupeds, birds, reptiles, fishes, mollusca, and radiata of the United Kingdom. Bell & Bradfute, J. Ducan, Edinburgh, London (xxiii + 565 pp.).
Forbes, E., Hanley, S., 1851. A history of British Mollusca and their shells. J. Conchol. 20, 150–151.
Friedberg, W., 1911–28. Mięczaki mioceńskie ziem Polskich (Mollusca Miocaenica Poloniae), 1. Ślimaki i łódkonogi, 1. Gastropoda et Scaphopoda. Lwow (Muzeum Imienia Dzieduszyckich) (1, 1–112 (1911). 2, 113–240 (1912). 3, 241–360 (1914). 4, 361–440 (1923). 5, 441–631 (1928)).
Fürsich, F.T., Oschmann, W., 1993. Shell beds as tools in basin analysis: the Jurassic of Kachchh, western India. J. Geol. Soc. Lond. 150, 169–185.
Gaspar, M.B., Castro, M., Monteiro, C.C., 1999. Effect of tooth spacing and mesh size on the catch of the Portuguese clam and razor clam dredge. ICES J. Mar. Sci. 56, 103–110.
George, L.M., Santiago, K.D., Palmer, T.A., Pollack, J.B., 2015. Oyster reef restoration: effect of alternative substrates on oyster recruitment and nekton habitat use. J. Coast. Conserv. 19, 13–22.
Goff, J., Chague-Goff, C., Nichol, S., Jaffe, B., Dominey-Howes, D., 2012. Progress in palaeotsunami research. Sediment. Geol. 243–244, 70–88.
Gray, J.E., 1840. Shells of molluscous animals. Synopsis of the contents of the British Museum 42nd ed. G. Woodfall, London, pp. 105–152.

Gray, J.E., 1847. A list of the genera of recent Mollusca, their synonyma and types. Proc. Zool. Soc. London 15, 129–219.
Gregory, M.R., 1991. New trace fossils from the Miocene of Northland, New Zealand: *Rorschachichnus amoeba* and *Piscichnus waitemata*. Ichnos 1, 195–205.
Guilding, L.V., 1834. Observations on Naticina and Dentalium, two genera of molluscous animals. Trans. Linn. Soc. Lond. 17, 29–35.
Harwell, H.D., 2010. Habitat complexity and habitat function of native (*Crassostrea virginica*) and non-native (*Crassostrea ariakensis*) oysters in the Chesapeake Bay region (PhD diss), Virginia Institute of Marine Science (202 pp.).
Harwell, H.D., Kingsley-Smith, P.R., Kellogg, M.L., Allen, S.M., Allen, S.K., Meritt, D.W., Paynter, K.T., Luckenbach, M.W., 2010. A comparison of *Crassostrea virginica* and *C. ariakensis* in Chesapeake Bay: does oyster species affect habitat function? J. Shellfish Res. 29, 253–269.
Harzhauser, M., Wessely, G., 2003. The Karpatian of the Korneuburg Basin (Lower Austria). In: Brzobohatý, R., Cicha, I., Kováč, M., Rögl, F. (Eds.), The Karpatian—A Lower Miocene Stage of the Central Paratethys. Masaryk University, Brno, pp. 107–110.
Harzhauser, M., Böhme, M., Mandic, O., Hofmann, Ch.-Ch., 2002. The Karpatian (Late Burdigalian) of the Korneuburg Basin—a palaeoecological and biostratigraphical synthesis. Beitr. Paläontol. 27, 441–456.
Harzhauser, M., Piller, W.E., Latal, C., 2007. Geodynamic impact on the stable isotope signatures in a shallow epicontinental sea. Terra Nova 19, 1–7.
Harzhauser, M., Sovis, W., Kroh, A., 2009. Das verschwundene Meer. 978-3-902421-42-5pp. 1–48 (Naturhistorisches Museum, Wien).
Harzhauser, M., Piller, W.E., Müllegger, S., Grunert, P., Micheels, A., 2010. Changing seasonality patterns in Central Europe from Miocene climate optimum to Miocene climate transition deduced from the *Crassostrea* isotope archive. Glob. Planet. Chang. 76, 77–84.
Hilber, V., 1879. Neue Conchylien aus den mittelsteirischen Mediterranschichten. Sitzungsber. Akad. Wiss. Math. Naturwiss. Cl. 79, 416–464.
Hoernes, R., Auinger, M., 1879–1891. Die Gasteropoden der Meeres-Ablagerungen der ersten und zweiten Miocänen Mediterran-Stufe in der Österreichisch-Ungarischen Monarchie. Abh. K.-Kg. Geol. Reichsanst. 12 (382 pp.).
Hmida, L., Ayache, N., Zohra Haouas, Z., Romdhane, M.S., 2010. Oocyte cohort analysis: criteria for an evaluation of the reproductive cycle in *Solen marginatus* (Pennánt, 1777), (Bivalvia: Solenacea) in Southern Tunisia. J. Shellfish Res. 29, 129–134.
Hölzel, M., Decker, K., Zámolyi, A., Strauss, P., Wagreich, M., 2010. Lower Miocene structural evolution of the central Vienna Basin (Austria). Mar. Pet. Geol. 27, 666–681.
Houbrick, R.S., 1992. Monograph of the genus *Cerithium* Bruguière in the Indo-Pacific (Cerithiidae: Prosobranchia). Smithson. Contrib. Zool. 510, 1–211.
Hörnes, M., 1851-1870. Die fossilen Mollusken des Tertiär-Beckens von Wien. Abh. K.-Kg. Geol. Reichsanst. 3–4 (479 pp.).
Jamabo, N., Chinda, A., 2010. Aspects of the ecology of *Tympanotonus fuscatus* var. *fuscatus* (Linnaeus, 1758) in the Mangrove Swamps of the Upper Bonny River, Niger Delta, Nigeria. Curr. Res. J. Biol. Sci. 2, 42–47.
Jurić, I., 2012. Age, growth and condition index of *Venerupis decussata* (Linnaeus, 1758) in the Eastern Adriatic Sea. Turk. J. Fish. Aquat. Sci. 12, 613–618.
Kazhdan, M., Bolitho, M., Hoppe, H., 2006. Poisson surface reconstruction. Proceedings of the Fourth Eurographics Symposium on Geometry Processing. 7, pp. 61–70.
Kennedy, V.S., Newell, R.I.E., Eble, A.F., 1996. The Eastern Oyster *Crassostrea virginica*. Maryland Sea Grant College, College Park, Maryland, USA (Publication UM-SG-TS-96-01).
Kern, A., Harzhauser, M., Mandic, O., Roetzel, R., Ćorić, S., Bruch, A.A., Zuschin, M., 2010. Millennial-scale vegetation dynamics in an estuary at the onset of the Miocene climate optimum. Palaeogeogr. Palaeoclimatol. Palaeoecol. 304, 247–261.
Kidwell, S.M., 1986. Models for fossil concentrations: paleobiologic implications. Paleobiology 12, 6–24.
Kidwell, S.M., 1991. The stratigraphy of shell concentrations. In: Allison, P.A., Briggs, D.E.G. (Eds.), Taphonomy, Releasing the Data Locked in the Fossil Record. Plenum Press, New York, pp. 211–290.
Kidwell, S.M., Bosence, D.W.J., 1991. Taphonomy and time-averaging of marine shelly faunas. In: Allison, P.A., Briggs, D.E.G. (Eds.), Taphonomy: releasing the data locked in the fossil recordTopics in Geobiology 9. Plenum Press, New York, pp. 115–209.
Kidwell, S.M., Tomašových, A., 2013. Implications of time-averaged death assemblages for ecology and conservation biology. Annu. Rev. Ecol. 44, 539–563.
Kirk, J., 2015. Advanced Dijkstra's Minimum Path Algorithm. http://www.mathworks.com/matlabcentral/fileexchange/20025-advanced-dijkstras-minimum-path-algorithm (last accessed 2015-04-02).
Kováč, M., Barath, I., Harzhauser, M., Hlavaty, I., Hudackova, N., 2004. Miocene depositional systems and sequence stratigraphy of the Vienna Basin. Cour. Forschungstinst. Senckenb. 246, 187–212.
Kulp, R.E., Politano, V., Lane, H.A., Lombardi, S.A., Paynter, K.T., 2011. Predation of juvenile *Crassostrea virginica* by two species of mud crabs found in the Chesapeake Bay. J. Shellfish Res. 30, 1–6.
Lahee, F.H., 1932. Bioherm and biostrome: geological notes. AAPG Bull. 16, 484.
Lamarck, J.P.B.A. de, 1809. Philosophie zoologique. Dentu, Paris (xxv + 428 pp.).
Lamarck, J.P.B.A. de, 1818. Histoire naturelle des animaux sans vertèbres. Tome cinquième. Deterville and Verdiere, Paris, pp. 411–612.
Lamarck, J.P.B.A. de Monet de, 1819. Histoire naturelle des animaux sans vertèbres. Tome sixième. 1re partie. Deterville and Verdiere, Paris (232 pp.).
Lamarck, J.B.P.A. de M., 1822. Histoire naturelle des animaux sans vertèbres, présentant des characters généraux et particuliers de ces animaux, leur distribution, leurs classes, leurs familles, leurs genres, ret la citation des principales espèces qui s'y rapportent, précédée dúne introduction offrant la détermination des caractères essentiels de l'animal, sa distinction du végétal et des autres corps naturels; enfin, l'exposition des principes fondamentaux de la zoologie, 7. de Lamarck, Paris (711 pp.).
Latal, C., Piller, W.E., Harzhauser, M., 2005. Shifts in oxygen and carbon isotope signals in marine molluscs from the Central Paratethys (Europe) around the Lower/Middle Miocene transition. Palaeogeogr. Palaeoclimatol. Palaeoecol. 231, 347–360.
Latal, C., Piller, W.E., Harzhauser, M., 2006. Small-scaled environmental changes: indications from stable isotopes of gastropods (Early Miocene, Korneuburg Basin, Austria). Int. J. Earth Sci. 95, 95–106.
Laurain, M., 1980. *Crassostrea gryphoides* et *C. gingensis* (Schlotheim, 1813) deux expressions morphologiques d'une même espèce (Miocène, Bivalvia). Geobios 13, 21–43.
Lazar, B., Gračan, R., Katić, J., Zavodnik, D., Jaklin, A., Tvrtković, N., 2011. Loggerhead sea turtles (*Caretta caretta*) as bioturbators in neritic habitats: an insight through the analysis of benthic molluscs in the diet. Mar. Ecol. 32, 65–74.
Lejart, M., Hily, C., 2011. Differential response of benthic macrofauna to the formation of novel oyster reefs (*Crassostrea gigas*, Thunberg) on soft and rocky substrate in the intertidal of the Bay of Brest, France. J. Sea Res. 65, 84–93.
Linnaeus, C., 1758. Systema naturae per regna tria naturae, secundum classes, ordines, genera, species, cum characteribus, differentiis, synonymis, locis. Editio decima, reformata. Tomus 1. Laurentii Salvii, Holmiae (824 pp.).
Mandic, O., Harzhauser, M., Roetzel, R., 2004a. Taphonomy and sequence stratigraphy of spectacular shell accumulation from the type stratum of the Central Paratethys stage Eggenburgian (Lower Miocene, NE Austria). Cour. Forschungstinst. Senckenb. 246, 69–88.
Mandic, O., Harzhauser, M., Schlaf, J., Piller, W.E., Schuster, F., Wielandt-Schuster, U., Nebelsick, J.H., Kroh, A., Rögl, F., Bassant, Ph., 2004b. Palaeoenvironmental reconstruction of an epicontinental flooding—Burdigalian (Early Miocene) of the Mut Basin (Southern Turkey). Cour. Forschungstinst. Senckenb. 248, 57–92.
Mayer, K., 1857. Description de Coquilles nouvelles des étages superieurs des terrains tertiaires. J. Conchyliologie 6, 176–187.
Mayer, K., 1858. Description de Coquilles nouvelles des étages superieurs des terrains tertiaires. J Conchyliologie 7, 187–193.
Mayer, M.C., 1868. Catalogue systématique et descriptif des fossiles des terrains tertiaires qui se trouvent au Musée Fédéral de Zurich. Troisième Cahier. Mollusques. Famille des Arcides. Librairie Schabelitz, Zurich (124 pp.).
Michelotti, G., 1847. Description des fossiles des terrains miocènes de l'Italie septentrionale. Ouvrage publié par la Société Hollandaise des Sciences, et accompagné d'un atlas de 17 planches. Naturkundige Verhandlingen van de Bataafsche Hollandsche Maatsechappye der Wetenschappen te Harlem 3. A. Arns & Compie, Leiden (408 pp.).
Milišić, N., 1991. Školjke i puževi Jadrana (Bivalves and Gastropods of the Adriatic Sea). Logos, Split (302 pp.).
Moneva, C.S.O., Baquiano, P.M.L., Blasco, J.O., Borlaza, K.M.E., Burias, D.M.E., Flores, K.A., Fuentes, G.R.E., Pancho, A.G.E., Sanchez, R.R.G., 2014. Comparative morphological descriptions of interior shell patterns of the venerid bivalves: *Meretrix lyrata, Mercenaria mercenaria* and *Venerupis philippinarum* using landmark-based geometric morphometric analysis. AACL Bioflux 7, 386–395.
Morton, R.A., Gelfenbaum, G., Jaffe, B.E., 2007. Physical criteria for distinguishing sandy tsunami and storm deposits using modern examples. Sediment. Geol. 200, 184–207.
Nothegger, C., Dorninger, P., 2009. 3D filtering of high-resolution Terrestrial Laser Scanner point clouds for cultural heritage documentation. Photogramm. Fernerkund. Geoinf. 1, 53–63.
Otepka, J., Ghuffar, S., Waldhauser, C., Hochreiter, R., Pfeifer, N., 2013. Georeferenced point clouds: a survey of features and point cloud management. ISPRS Int. J. Geo-Inf. 2, 1038–1065.
Parker, R., 1955. Changes in the invertebrate fauna, apparently attributable to salinity changes, in the bays of central Texas. J. Paleontol. 29, 193–211.
Patzkowsky, M.E., Holland, S.M., 2012. Stratigraphic paleobiology—understanding the distribution of fossil taxa in time and space. Univ. of Chicago Press (259 pp.).
Pearson, N.J., Gingras, M.K., Armitage, I.A., Pemberton, S.G., 2007. Significance of Atlantic sturgeon feeding excavations, Mary's Point, Bay of Fundy, New Brunswick, Canada. Palaios 22, 457–464.
Pennant, T., 1777. British zoology. Volume IV. Crustacea, Mollusca, Testacea. Benjamin White, London (VIII + 154 pp.).
Pervesler, P., Roetzel, R., Uchman, A., 2011. Ichnology of shallow sublittoral siliciclastics of the Burgschleinitz Formation (Lower Miocene, Eggenburgian) in the Alpine-Carpathian Foredeep (NE Austria). Aust. J. Earth Sci. 104, 81–96.
Pfeifer, N., Mandlburger, G., Otepka, J., Karel, W., 2014. OPALS—a framework for airborne laser scanning data analysis. Comput. Environ. Urban. Syst. 45, 125–136.
Philippi, R.A., 1836. Enumeratio molluscorum Siciliae cum viventium tum in tellure tertiaria fossilium, quae in itinere suo observavit. 1. Schropp, Berolini (XIV + 267 pp.).
Powell, E.N., Kraeuter, J.N., Ashton-Alcox, K.A., 2006. How long does oyster shell last on an oyster reef? Estuar. Coast. Shelf Sci. 69, 531–542.
Powell, E.N., Klinck, J.M., Ashton-Alcox, K., Hofmann, E.E., Morson, J., 2012. The rise and fall of *Crassostrea virginica* oyster reefs: the role of disease and fishing in their demise and a vignette on their management. J. Mar. Res. 70, 505–558.
Pulteney, R., 1799. Catalogues of the birds, shells, and some of the more rare plants, of Dorsetshire. From the new and enlarged edition of Mr. Hutchins's history of that county. Nichols, London (92 pp.).
Pusch, G.G., 1836–1837. Polens Paläontologie oder Abbildung und Beschreibung der vorzüglichsten und der noch unbeschriebenen Petrefakten aus den Gebirgsformationen in Polen, Volhynien und den Karpathen nebst einigen allgemeinen Beiträgen zur Petrefaktenkunde und einem Versuch zur Vervollständigung der Geschichte des europäischen Auer-Ochsen. E. Schweizerbart's Verlagshandlung, Stuttgart (218 pp.).

Quan, W., Zhu, J., Ni, Y., Shi, L., Chen, Y., 2009. Faunal utilization of constructed intertidal oyster (*Crassostrea rivularis*) reef in the Yangtze River estuary, China. Ecol. Eng. 35, 1466–1475.
Rafinesque, C.S., 1815. Analyse de la nature ou tableau de l'univers et des corps organisés. Le nature es mon guide, et Linnéus mon maître. privately published, Palermo (224 pp.).
Reid, D.G., Dyal, P., Lozouet, P., Glaubrecht, M., Williams, S.T., 2008. Mudwhelks and mangroves: the evolutionary history of an ecological association (Gastropoda: Potamididae). Mol. Phylogenet. Evol. 47, 680–699.
Risso, A., 1826. Histoire naturelle des principales productions de l'Europe méridionale et particulièrement de celles des environs de Nice et des Alpes Maritimes, Tome quatrième. Levrault, Paris (VII + 492 pp.).
Rögl, F., 1998. Foraminiferenfauna aus dem Karpat (Unter-Miozän) des Korneuburger Beckens. Beitr. Paläontol. 23, 123–173.
Romero, S.M.B., Moreira, G.S., 1980. The combined effects of salinity and temperature on the survival of embryos and veliger larvae of *Perna perna* (Linne, 1758) (Mollusca-Bivalvia). Bol. Fisiol. Anim. 5, 45–58 (São Paulo).
Rufino, M.R., Gaspar, M.B., Pereira, A.M., Maynou, F., Monteiro, C.C., 2010. Ecology of megabenthic bivalve communities from sandy beaches on the south coast of Portugal. Sci. Mar. 74, 163–178.
Sacco, F., 1894. I molluschi dei terreni terziarii del Piemonte e della Liguria. Parte 16: Fam. Cancellariidae H. e A. Adams 1853. Boll. Mus. Zool. Anat. Comp. Reale Univ. Torino 9 (70 pp).
Scheffers, A., Kelletat, D., 2003. Sedimentologic and geomorphologic tsunami imprints worldwide—a review. Earth Sci. Rev. 63, 83–92.
Schlotheim, E.F. Baron von, 1813. Beiträge zur Naturgeschichte der Versteinerungen in geognostischer Hinsicht. In: Leonhard, C.C. (Ed.), Leonhard's Taschenbuch für die gesammte Mineralogie mit Hinsicht auf die neuesten Entdeckungen (series 1). 7, pp. 1–134.
Seilacher, A., Gishlick, A.D., 2014. Morphodynamics. CRS Press (551 pp.).
Seilacher, A., Matyja, B.A., Wierzbowski, A., 1985. Oyster beds: morphologic response to changing substrate conditions. Lect. Notes Earth Sci. 1, 421–435.
Shanmugam, G., 2006. The tsunamite problem. J. Sediment. Res. 76, 718–730.
Shanmugam, G., 2012. Process-sedimentological challenges in distinguishing paleotsunami deposits. Nat. Hazards 63, 5–30.
Das Karpat des Korneuburger Beckens, Teil 1. In: Sovis, W., Schmid, B. (Eds.), Beiträge zur Paläontologie 23, pp. 1–413.
Das Karpat des Korneuburger Beckens, Teil 2. In: Sovis, W., Schmid, B. (Eds.), Beiträge zur Paläontologie 27, pp. 1–467.
Smith, J., 1847. On the age of the tertiary Beds of the Tagus with a catalogue of the fossils. Q. J. Geol. Soc. London 3, 410–423.
Sowerby II, G.B., 1832–1841. The conchological illustrations, or coloured figures of all the hitherto unfigured Recent shells. privately published, London (200 plates).
Stenzel, H.B., 1971. Oysters. Treatise on Invertebrate Paleontology N/3. pp. 953–1224.
Stiner, J., 2006. Predation on the eastern oyster *Crassostrea virginica* on intertidal reefs affected by recreational boating (M.S. Thesis), University of Central Florida, Orlando, Florida (114 pp.).
Strayer, D.L., Powell, J., Ambrose, P., Smith, L.C., Pace, M.L., Fischer, D.T., 1996. Arrival, spread, and early dynamics of a zebra mussel (*Dreissena polymorpha*) population in the Hudson River estuary. Can. J. Fish. Aquat. Sci. 53, 1143–1149.
Thomsen, M.S., Silliman, B.R., McGlathery, K.J., 2007. Spatial variation in recruitment of native and invasive sessile species onto oyster reefs in a temperate soft-bottom lagoon. Estuar. Coast. Shelf Sci. 72, 89–101.
Thunberg, C.P., 1793. Tekning och Beskrifning på en stor Ostronsort ifrån Japan. Kongliga Vetenskaps Academiens Nya Handlingar 14, 140–142.
Tomašových, A., Fürsich, F.T., Olszewski, T.D., 2006. Modeling shelliness and alteration in shell beds: variation in hardpart-input and burial rates leads to opposing predictions. Paleobiology 32, 278–298.
Vakily, J.M., 1989. The biology and culture of mussels of the genus *Perna*. International Center for Living Aquatic Resources Management Studies and Reviews 17. ICLARM, Manila (63 pp.).
van der Zee, E.M., van der Heide, T., Donadi, S., Eklöf, J.S., Eriksson, B.K., Olff, H., van der Veer, H.W., Piersma, T., 2012. Spatially extended habitat modification by intertidal reef-building bivalves has implications for consumer-resource interactions. Ecosystems 15, 664–673.
Voronoi, G., 1908. Nouvelles applications des paramètres continus à la théorie des formes quadratiques. Deuxième mémoire. Recherches sur les parallélloèdres primitifs. J. Reine Angew. Math. 133, 97–178.
Waldbusser, G.G., Steenson, R.A., Gren, M.A., 2011. Oyster shell dissolution rates in estuarine waters: effects of pH and shell legacy. J. Shellfish Res. 30, 659–669.
Wells, F.E., 2003. Aspects of the ecology of the mudwhelks *Terebralia palustris* and *T. semistriata* in northwestern Australia. The marine flora and fauna of Dampier, Western Australia: proceedings of the Twelfth International Marine Biological Workshop: held in Dampier from 24 July to 11 August 2000, organised by Western Australian Museum, the University of Western Australia, Western Australian Branch, Australian Marine Sciences Association. vol. 1, pp. 193–208
Wessely, G., 1998. Geologie des Korneuburger Beckens. Beitr. Paläontol. 23, 9–23.
Whitman, E.R., Reidenbach, M.A., 2012. Benthic flow environments affect recruitment of *Crassostrea virginica* larvae to an intertidal oyster reef. Mar. Ecol. Prog. Ser. 463, 177–191.
Willan, R.C., 2013. A key to the potamidid snails (longbums, mudcreepers and treecreepers) of northern Australia. North. Territ. Nat. 24, 68–80.
Zuschin, M., Harzhauser, M., Mandic, O., 2004. Palaeoecology and taphonomy of a single parautochthonous Paratethyan tidal flat deposit (Karpatian, Lower Miocene—Kleinebersdorf, Lower Austria). Courier Forschungsinstitut Senckenberg 246, 153–168.
Zuschin, M., Harzhauser, M., Mandic, O., 2005. Influence of size-sorting on diversity estimates from tempestitic shell beds in the middle Miocene of Austria. Palaios 20, 142–158.
Zuschin, M., Harzhauser, M., Mandic, O., 2007. The stratigraphic framework of fine-scale gradual and disjunct faunal replacements in the Middle Miocene of the Vienna basin (Austria). Palaios 22, 286–297.
Zuschin, M., Harzhauser, M., Hengst, B., Mandic, O., Roetzel, R., 2014. Long-term ecosystem stability in an Early Miocene estuary. Geology 42, 1–4.